Electronic Supplementary Information (ESI) for

Vinylene-bridged donor-acceptor type porous organic polymers for enhanced photocatalysis of amine oxidative coupling reactions under visible light

Bang Wu,[a] Xinyue Jiang,[a] Yang Liu,[a] Qiu-Yan Li,*[a] Xinsheng Zhao[b] and Xiao-Jun Wang*[a]

[a]*Jiangsu Key Laboratory of Green Synthetic Chemistry for Functional Materials, School of Chemistry and Materials Science, Jiangsu Normal University, Xuzhou 221116, P. R. China*

[b]*School of Physics and Electronic Engineering, Jiangsu Normal University, Xuzhou 221116, P. R. China.*

E-mail: xjwang@jsnu.edu.cn; qyli@jsnu.edu.cn

General method and materials

Unless specifically mentioned, all chemicals are commercially available and were used as received. The precursor compounds tricyanomesitylene (TCM) and tris[1-(1'-formyl-4,4'-biphenyl)]amine (TFBA) were prepared according to the reported literature methods.[S1] ^{1}H and ^{13}C NMR spectra were taken on a Bruker AV400 at room temperature. High-resolution mass spectrometry (HR-MS) was performed on a Thermo ultimate Q-Exactive in positive mode. ^{13}C cross-polarization/magic angle spinning solid-state nuclear magnetic resonance (CP/MAS ssNMR) experiments were performed on a Bruker AVANCE III 400 WB spectrometer operating at 100.62 MHz for ^{13}C using a double resonance 4 mm MAS NMR probe and a sample spinning rate of 6 kHz. The powder X-ray diffraction measurements were taken on a Bruker D8 diffractometer using Cu-K_α radiation (λ = 1.5418 Å) at room temperature. Low-pressure gas sorption measurements were performed by using Quantachrome Instruments Autosorb-iQ with the extra-high pure gases. Brunauer-Emmett-Teller (BET) surface area and pore size distribution were calculated from the N_2 sorption isotherms at 77 K based on Non-Local Density Functional Theory (NL-DFT) model in the Quantachrome ASiQwin 2.01 software package. UV-vis diffuse reflectance spectra (UV-vis DRS) were recorded at room temperature on an Agilent Cary 7000 Spectrophotometer. Photoluminescence (PL) spectra were obtained with an Edinburgh FLS920 spectrophotometer. The infrared spectra were recorded on a Thermo Scientific Nicolet iS10 FT-IR spectrometer as KBr pellets. Thermal gravimetric analyses (TGA) were performed on a TA-Q50 thermoanalyzer thermogravimetric analyzer in nitrogen atmosphere from 45 °C to 800 °C at the rate of 10 °C min^{-1}. Ultraviolet photoelectron spectroscopy (UPS) was performed on Thermo Scientific Escalab 250Xi. Field-emission scanning electron microscopy (FE-SEM) images were obtained on a HITACHI S-8010 instrument operating at 10 kV.

Synthesis and Characterizations

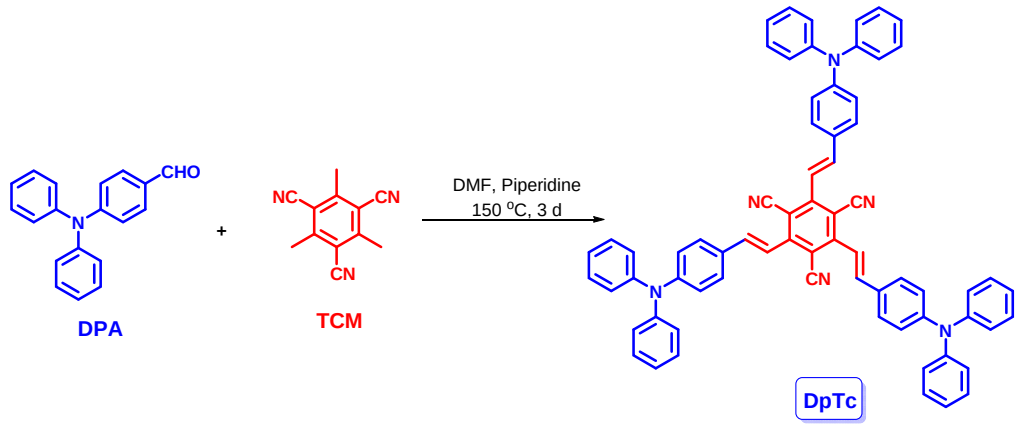

Scheme S1. Synthesis of model compound **DpTc**.

Model Compound **DpTc**: TCM (195mg, 1.0 mmol), DPA (1.23g, 4.5 mmol) and piperidine (511 mg, 6 mmol) were added into 20 mL anhydrous DMF under the protection of nitrogen. The reaction mixture was heated to 150 °C and stirred for 72 hours under nitrogen atmosphere. After that, the solution was poured into water and extracted with dichloromethane, dried over Na_2SO_4, and concentrated to obtain a henna solid. The crude product was purified by column chromatography over a silica gel column using petroleum ether-dichloromethane (v/v, 1.2/1) as the eluent to afford model compound as a red solid (356 mg, 0.37 mmol, yield: 37%). ^{1}H NMR (400 MHz, $CDCl_3$) δ 7.71 (d, J = 16.3 Hz, 3H), 7.49 (d, J = 8.6 Hz, 6H), 7.30 (t, J = 7.8 Hz, 15H), 7.20 – 7.00 (m, 24H). ^{13}C NMR (101 MHz, $CDCl_3$) δ 150.11, 149.28, 147.05, 141.97, 129.65, 129.24, 128.40, 125.52, 124.18, 122.09, 118.67, 116.29, 107.56. ESI-HRMS: *m/z* calcd for $C_{69}H_{49}N_6$: 961.4013, found: 961.3977 $[M+H]^+$.

Procedure for the synthesis of **TpTc-POP**: TCM (98 mg, 0.5 mmol), TFPA (165 mg, 0.5 mmol) and piperidine (256 mg, 3 mmol) were ultrasonically dissolved in 10 mL of DMF in a 20 mL Teflon-lined stainless-steel autoclave. The vessel was tightly sealed and heated in an oven of 150 °C for 72 h. After cooling down to RT, the solid was collected, washed with anhydrous DMF, acetone and DCM. Then, the solid was Soxhlet extracted with THF for 24 h and was dried under vacuum for 12 h at 80 °C to give red powder in 92% yield.

Procedure for the synthesis of **TbTc-POP**: TCM (49 mg, 0.25 mmol), TFBA (144 mg, 0.25 mmol) and piperidine (639 mg, 7.5 mmol) were ultrasonically dissolved in 10 mL of DMF in a 20 mL Teflon-lined stainless-steel autoclave. The vessel was tightly sealed and heated in an oven of 150 ^{o}C for 72 h. After cooling down to RT, the solid was collected, washed with anhydrous DMF, acetone and DCM. Then, the solid was Soxhlet extracted with THF for 24 h and was dried under vacuum for 12 h at 80 ^{o}C to give red powder in 89% yield.

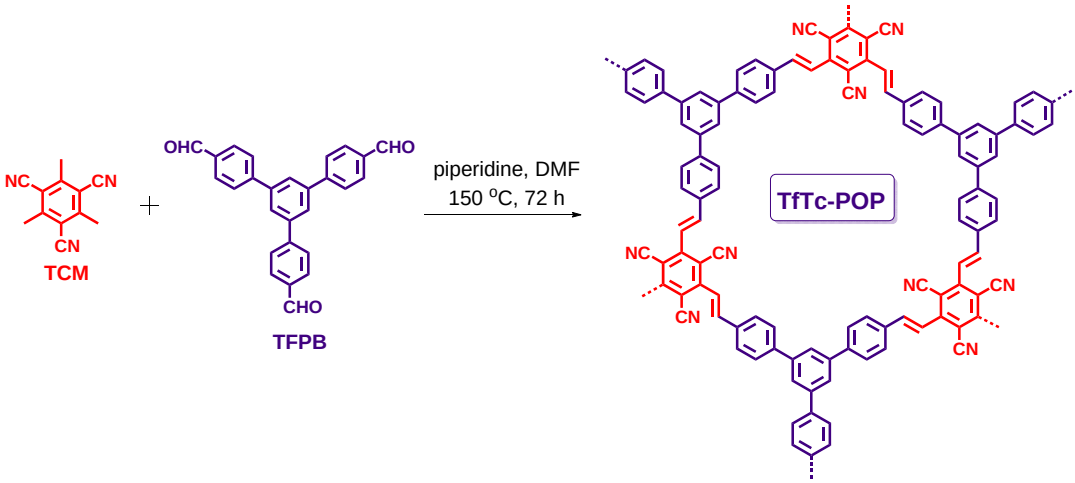

Scheme S2. Synthesis of control POP **TfTc-POP**.

Control POP **TfTc-POP**: TCM (98 mg, 0.5 mmol), TFPB (195 mg, 0.5 mmol) and piperidine (256 mg, 3 mmol) were ultrasonically dissolved in 10 mL of DMF in a 20 mL Teflon-lined stainless-steel autoclave. The vessel was tightly sealed and heated in an oven of 150 ^{o}C for 72 h. After cooling down to RT, the solid was collected, washed with anhydrous DMF, acetone and DCM. Then, the solid was Soxhlet extracted with THF for 24 h and was dried under vacuum for 12 h at 80 ^{o}C to give brown powder in 91% yield.

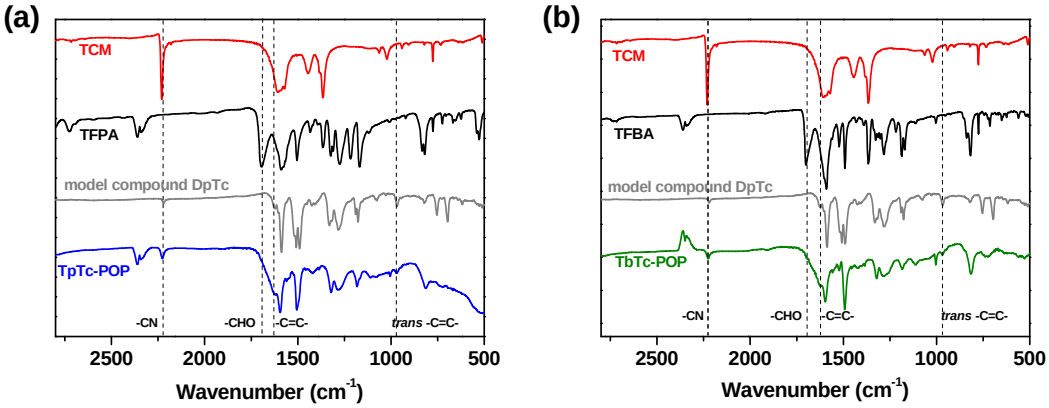

Fig. S1 The FT-IR comparison of TpTc-POP (a), TbTc-POP (b) and their corresponding monomers as well as model compound DpTc.

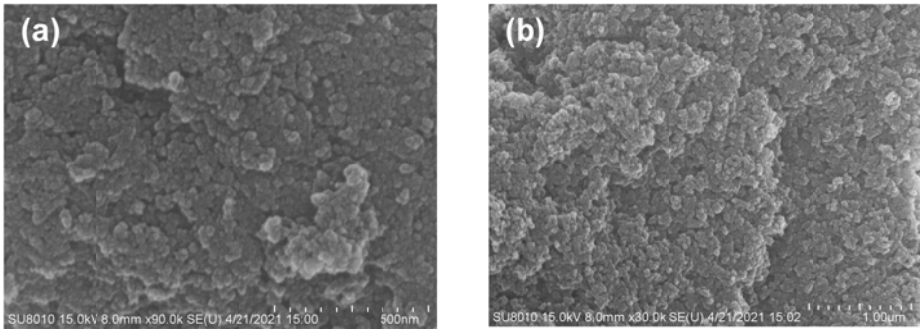

Fig. S2 SEM images of TpTc-POP (a) and TbTc-POP (b).

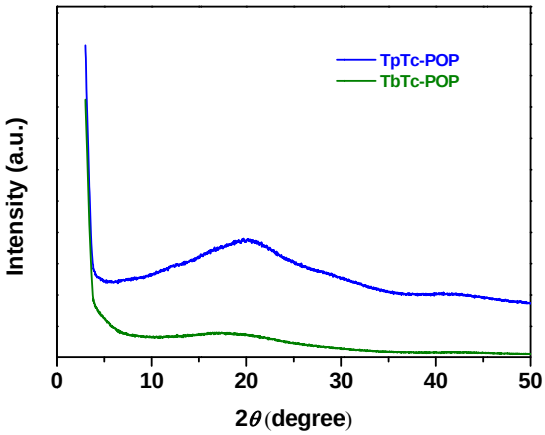

Fig. S3 PXRD patterns of TpTc-POP and TbTc-POP.

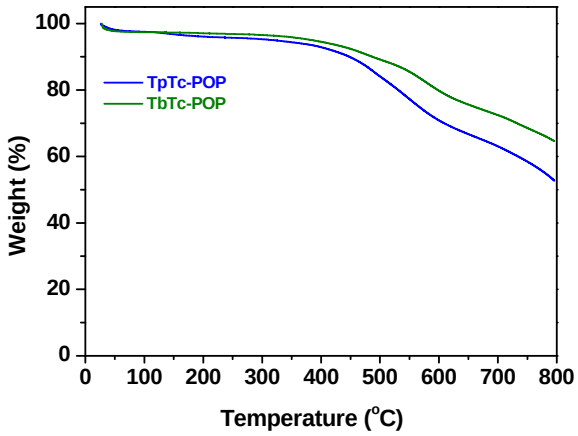

Fig. S4 TGA of TpTc-POP and TbTc-POP under N_2 atmosphere with a heating rate of 10 °C/min.

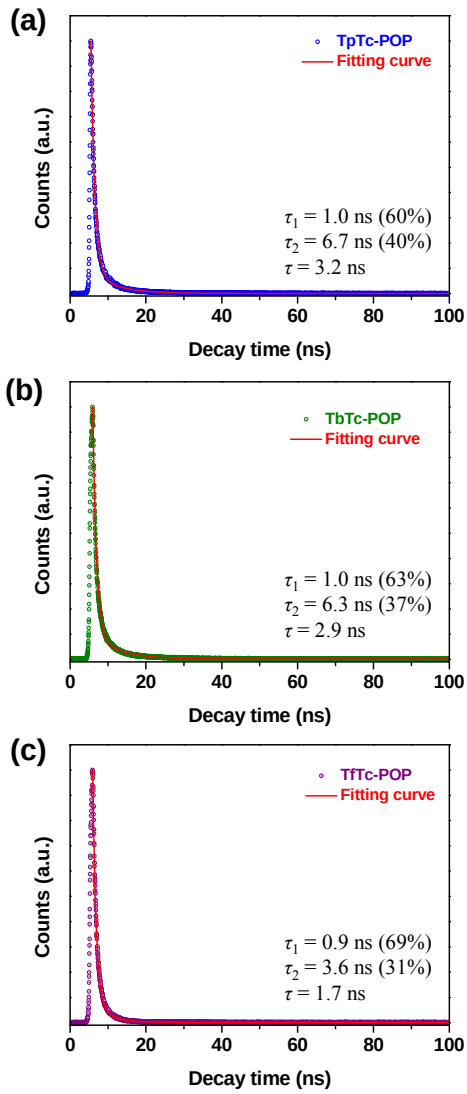

Fig. S5 PL decay spectra of TpTc-POP (a), TbTc-POP (b) and TfTc-POP (c). The traces can be

fitted with two-exponential decays (solid lines) $I(t) = A + B_1 e^{-t/\tau 1} + B_2 e^{-t/\tau 2}$, where A is a constant, B_1 and B_2 are pre-exponential factors; τ_1 and τ_2 are the fitted time constants of the decays. The fluorescence lifetime was calculated according to $\tau = (B_1\tau_1^2+B_2\tau_2^2)/(B_1\tau_1+B_2\tau_2)$.

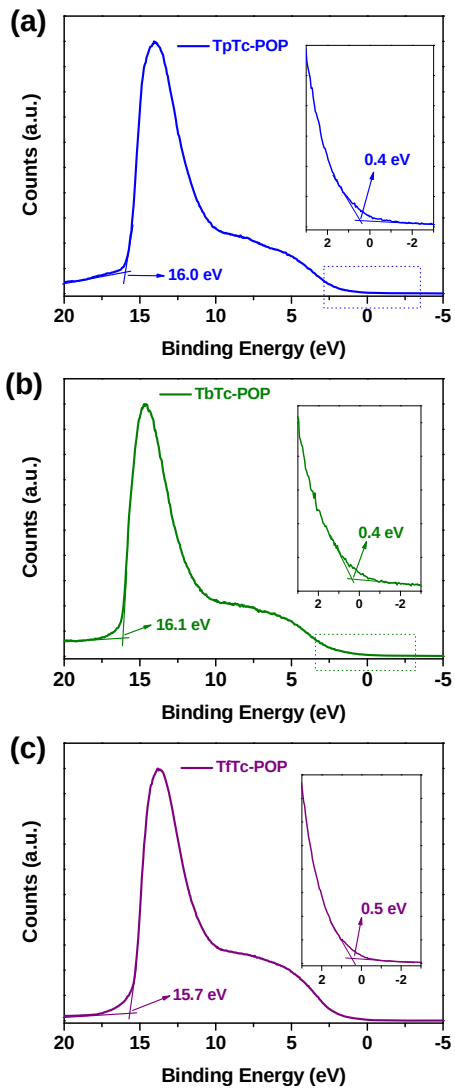

Fig. S6 High-resolution valence band ultraviolet photoelectron spectra (UPS) of TpTc-POP (a), TbTc-POP (b) and control TfTc-POP (c).

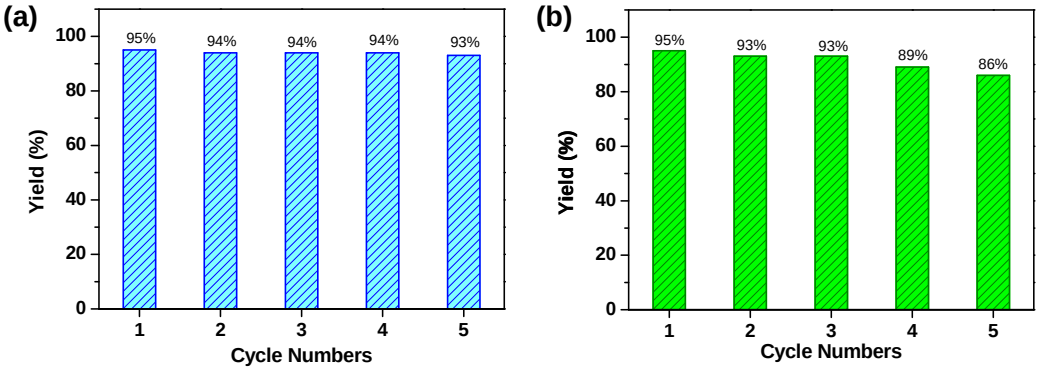

Fig. S7 Recycling of TpTc-POP (a) and TbTc-POP (b) for the photocatalyzed aerobic oxidative coupling of benzylamine to imine.

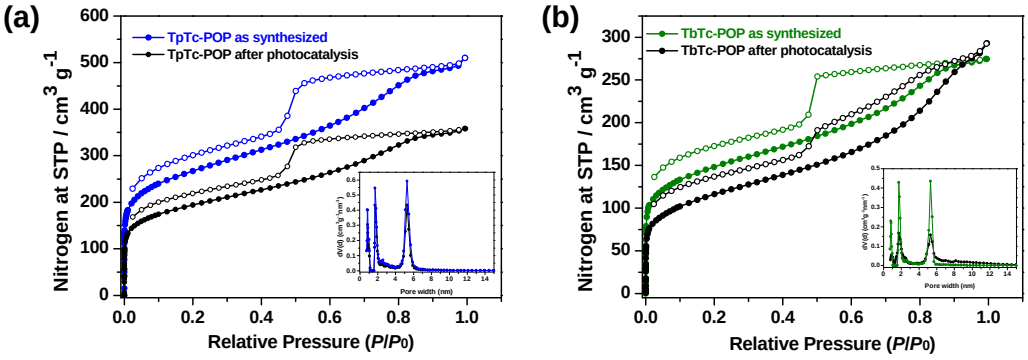

Fig. S8 Nitrogen sorption isotherms for as-synthesized and after-photocatalytic porous polymers TpTc-POP (a) and TbTc-POP (b).

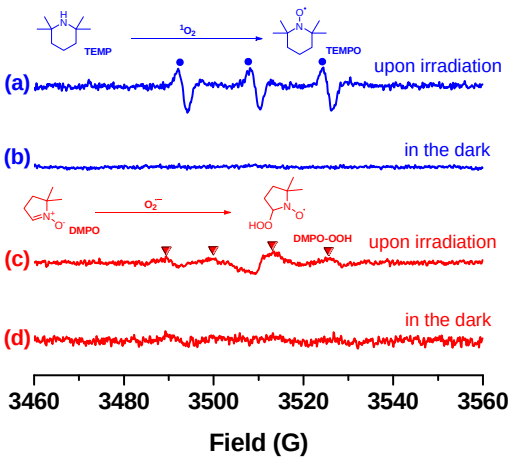

Fig. S9 EPR spectra of a mixture of TpTc-POP in CH_3CN with TEMP upon light irradiation (a) and in the dark (b) as well as DMPO upon light irradiation (c) and in the dark (d).

Table S1 Photocatalytic oxidative coupling of various amines by TbTc-POP[a]

Entry	Substrate	Product	Time (h)	Yield[b] (%)
1	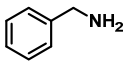	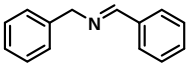	8	95
2	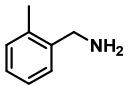	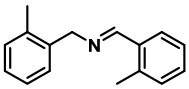	8	94
3	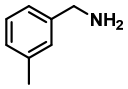	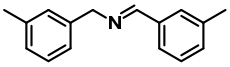	8	92
4	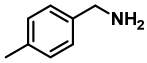	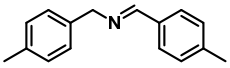	8	99
5	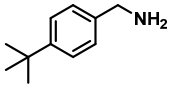	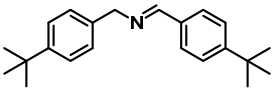	8.5	95
6	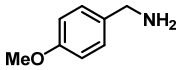	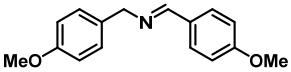	8	97
7	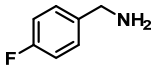	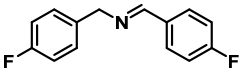	8	99
8	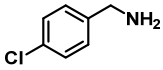	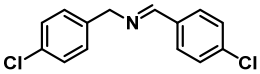	8	95
9	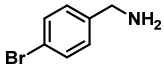	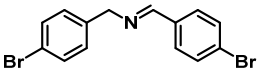	6	90
10	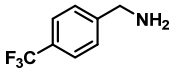	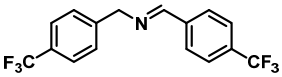	10.5	87
11	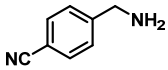	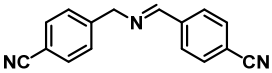	16	99
12	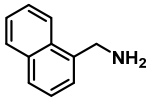	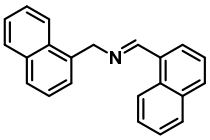	10.5	96
13	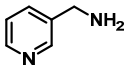	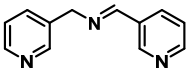	10.5	93
14	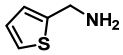	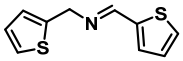	10.5	91

[a]Reaction conditions: benzylamines (0.5 mmol), TpTc-POP (6 mg), CH_3CN (1 mL), irradiation with white LEDs (3W, ~100 mW cm^{-2}). [b]Determined by ^1H NMR analysis.

Table S2 Comparison of reported various POPs for photocatalyzing oxidative coupling reactions of benzylamine.

System	Linkage	Crystalline	S_{BET} (m^2 g^{-1})	Light Source	Solvent	Time & Yield	Ref.
TpTc-POP	-CH=CH-[a]	No	966	white LEDs	CH_3CN	6 h, 95%	This study
TbTc-POP	-CH=CH-[a]	No	538	white LEDs	CH_3CN	8 h, 95%	
CF-HCP	$-CH_2-$	No	1217	green LEDs	CH_3CN	6 h, 91%	S2
Py-BSZ-COF	-CH=C(CN)-[b]	Yes	600	520 nm LEDs	CH_3CN	12 h, 99%	S3
A-CTF-2	acetylene	No	24	300 W xenon lamp	CH_3CN	4 h, 98%	S4
PyTz-COF	-C=N-	Yes	1175	white LEDs	CH_3CN+H_2O	2 h, 90%	S5
Por-sp^2c-COF	-CH=C(CN)-[b]	Yes	714	red LEDs	CH_3CN	15 min, 94%[c]	S6
pTCT	triazine	No	797	white CFL	CH_3CN	12 h, 97%	S7
B-BT	acetylene	No	689	blue LEDs	CH_3CN	3 h, 74%	S8
B-BO-1,3,5	acetylene	No	474	blue LEDs	CH_3CN	3 h, 48%	S9
CzBDP	alkyl	No	180	9 W CFL	CH_3CN	15 h, 75%	S10

[a]unsubstituted vinylene -CH=CH-, [b]substituted acrylonitrile -CH=C(CN)-, [c]cooperative photocatalysis with TEMPO.

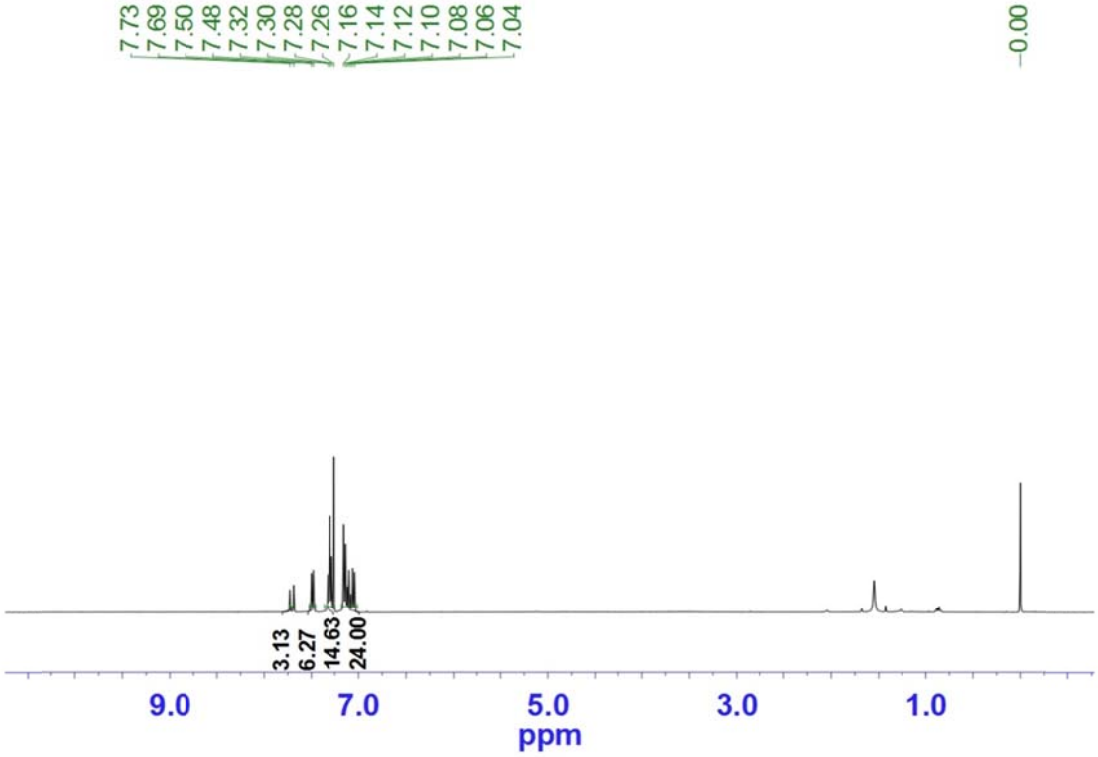

Fig. S10 ^{1}H NMR of model compound **DpTc** (400 MHz, $CDCl_3$)

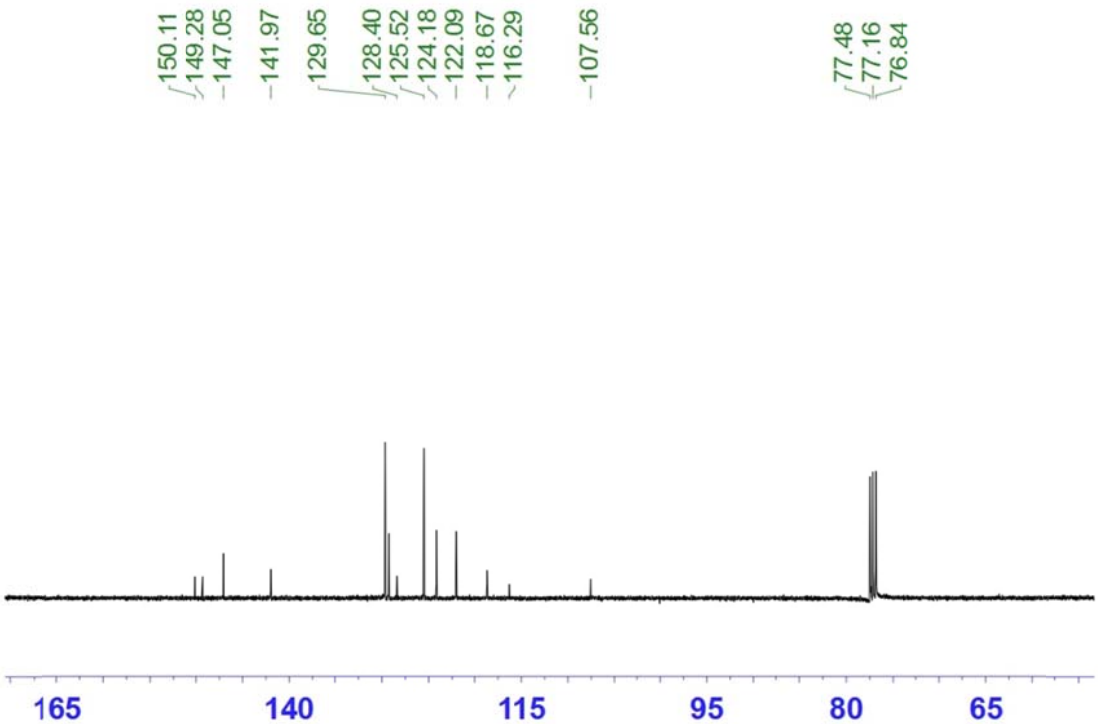

Fig. S11 ^{13}C NMR of model compound **DpTc** (101 MHz, $CDCl_3$).

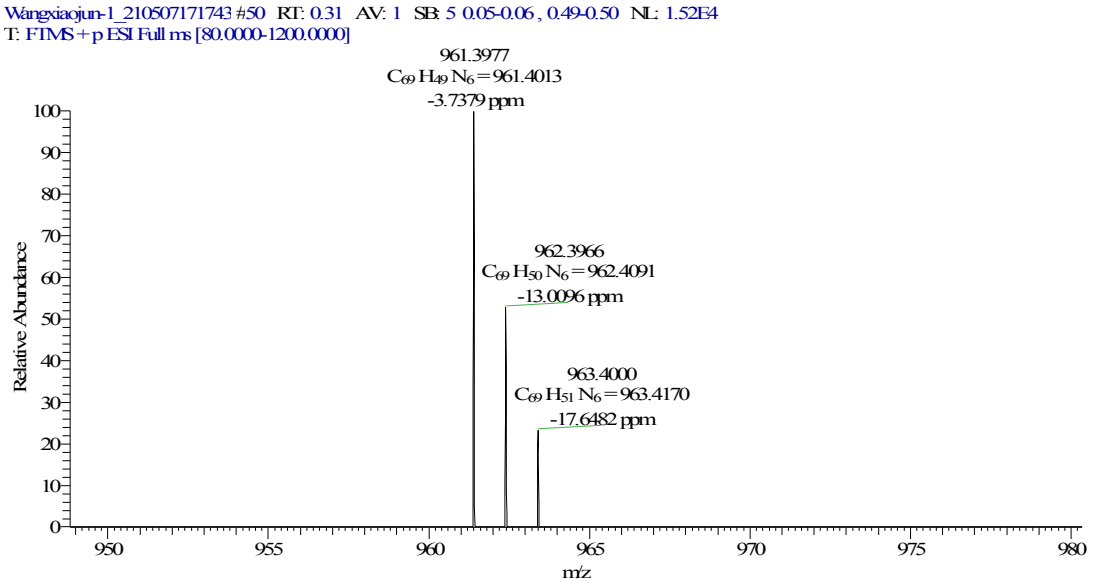

Fig. S12 ESI-HRMS spectra of model compound **DpTc**.

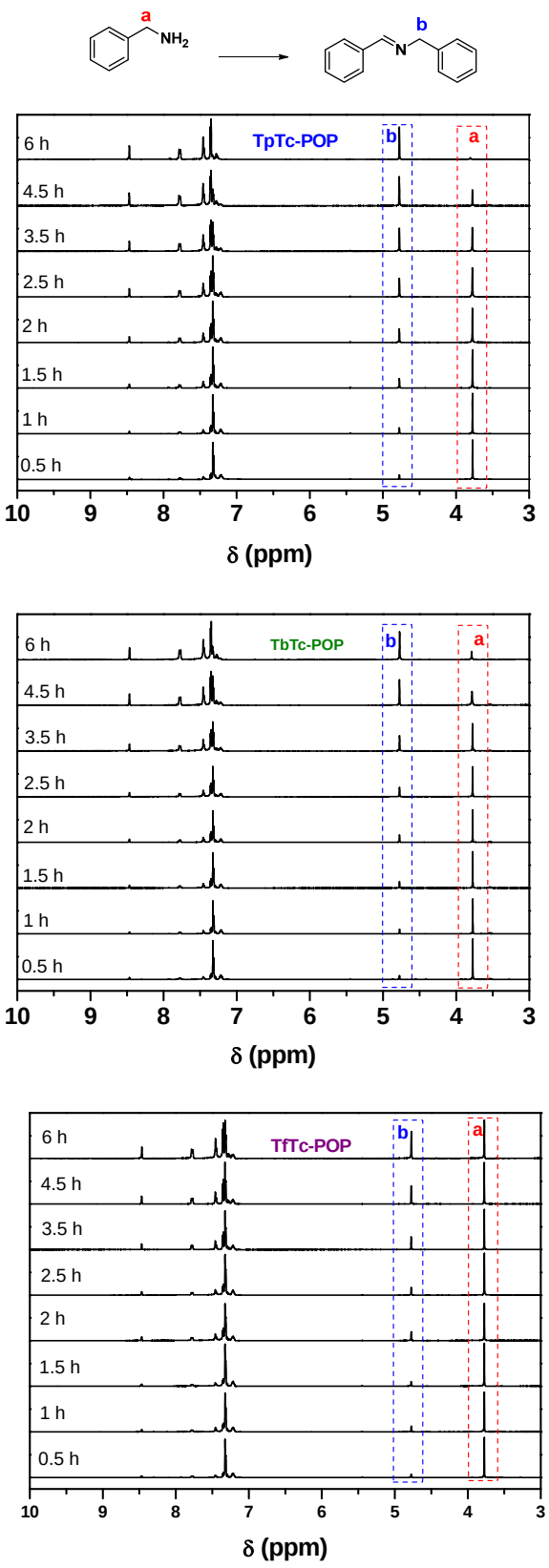

Fig. S13 Time dependent ^{1}H NMR spectra of photocatalytic oxidative coupling reaction of benzylamine to imine by using different POPs (TpTc-POP, TbTc-POP and TfTc-POP) under the irradiation of white-LEDs in an open air atmosphere.

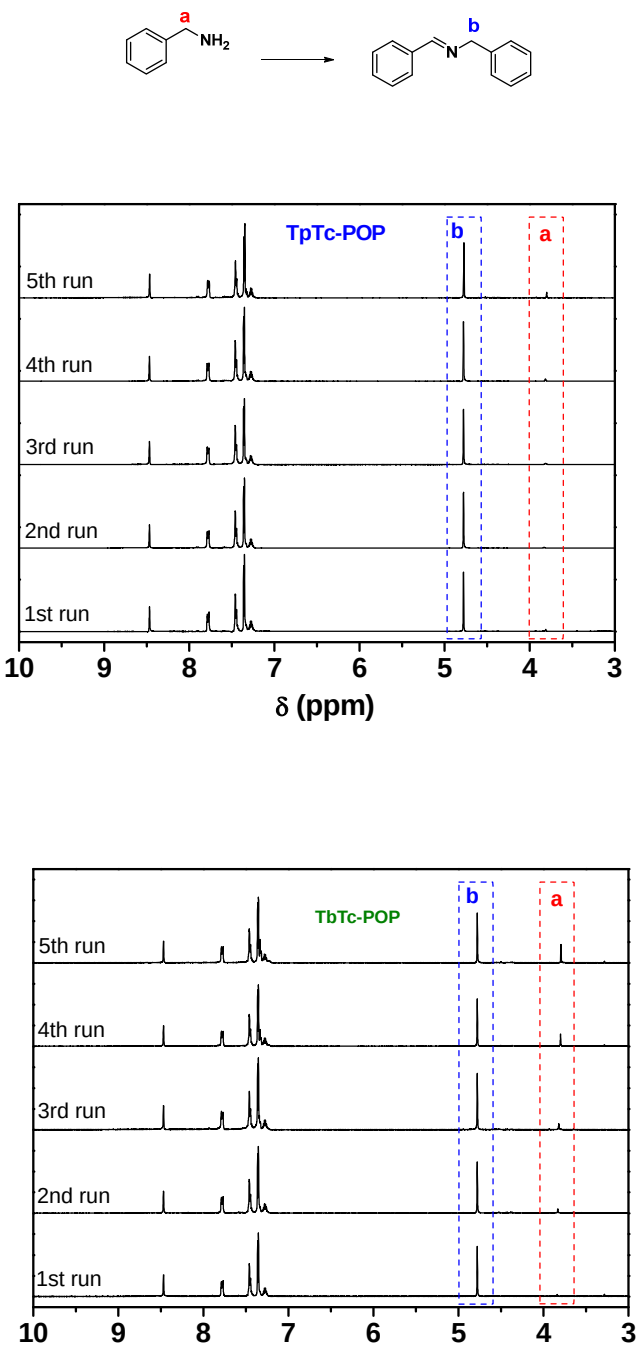

Fig. S14 Successive ^{1}H NMR spectra of photocatalytic oxidative coupling reaction of benzylamine to imine by recycling POPs (TpTc-POP and TbTc-POP) under the irradiation of white-LEDs in an open air atmosphere.

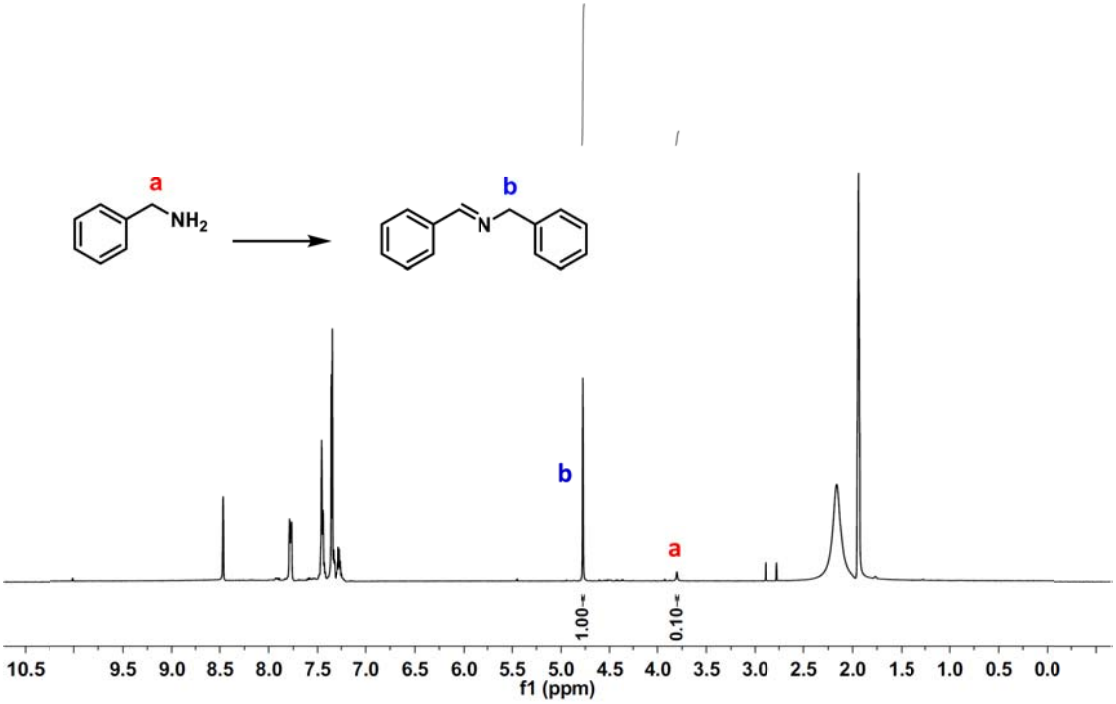

Fig. S15 ^{1}H NMR of the reaction mixture after photocatalysis by TpTc-POP (Entry 1, Table 1).

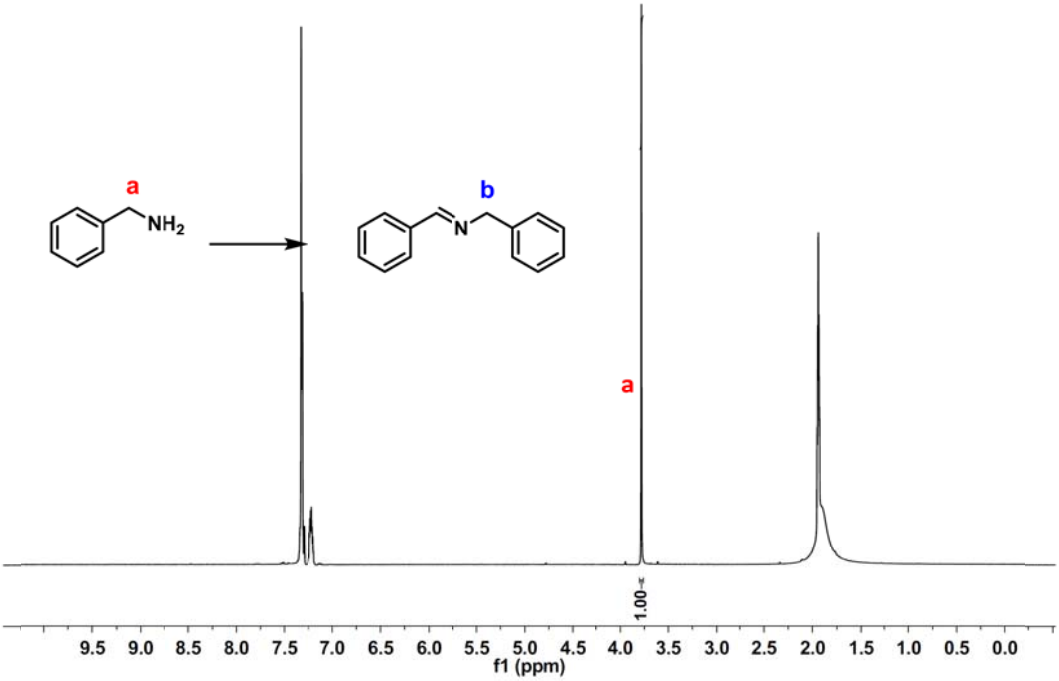

Fig. S16 ^{1}H NMR of the reaction mixture (Entry 2, Table 1).

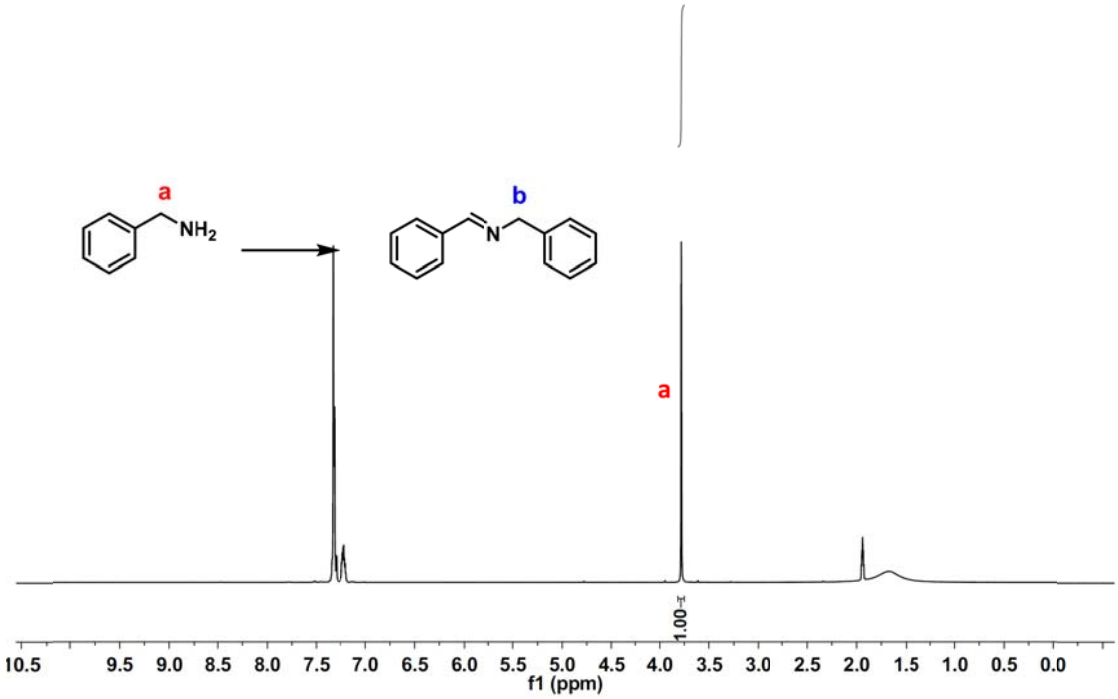

Fig. S17 ^{1}H NMR of the reaction mixture (Entry 3, Table 1).

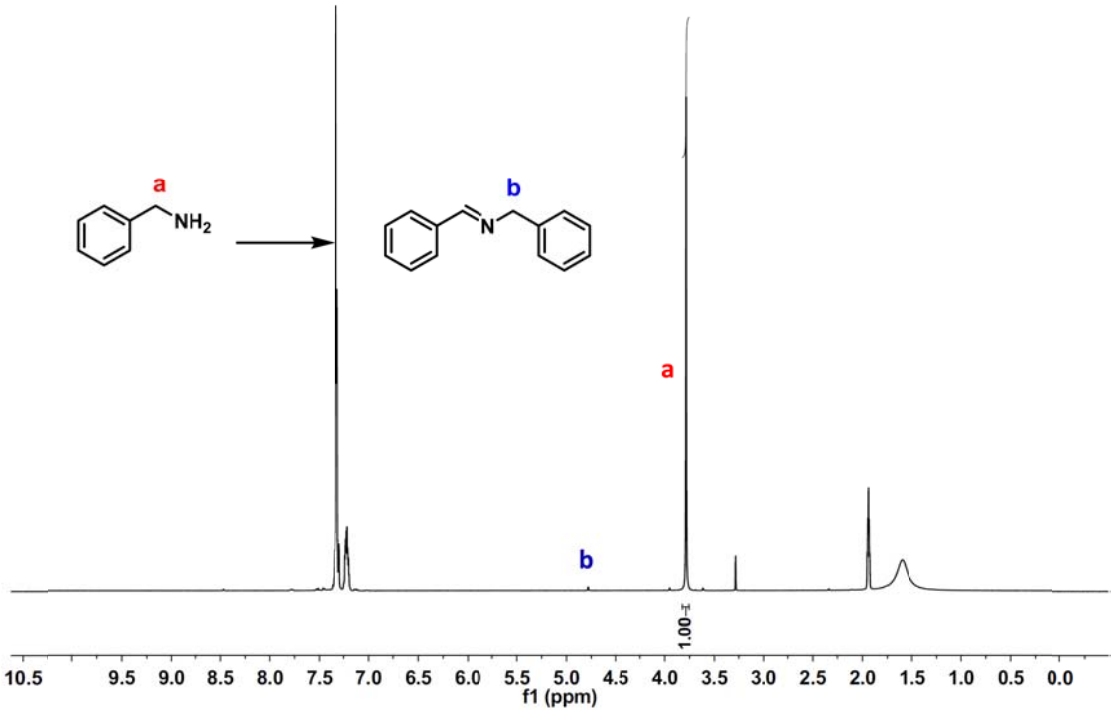

Fig. S18 ^{1}H NMR of the reaction mixture (Entry 4, Table 1).

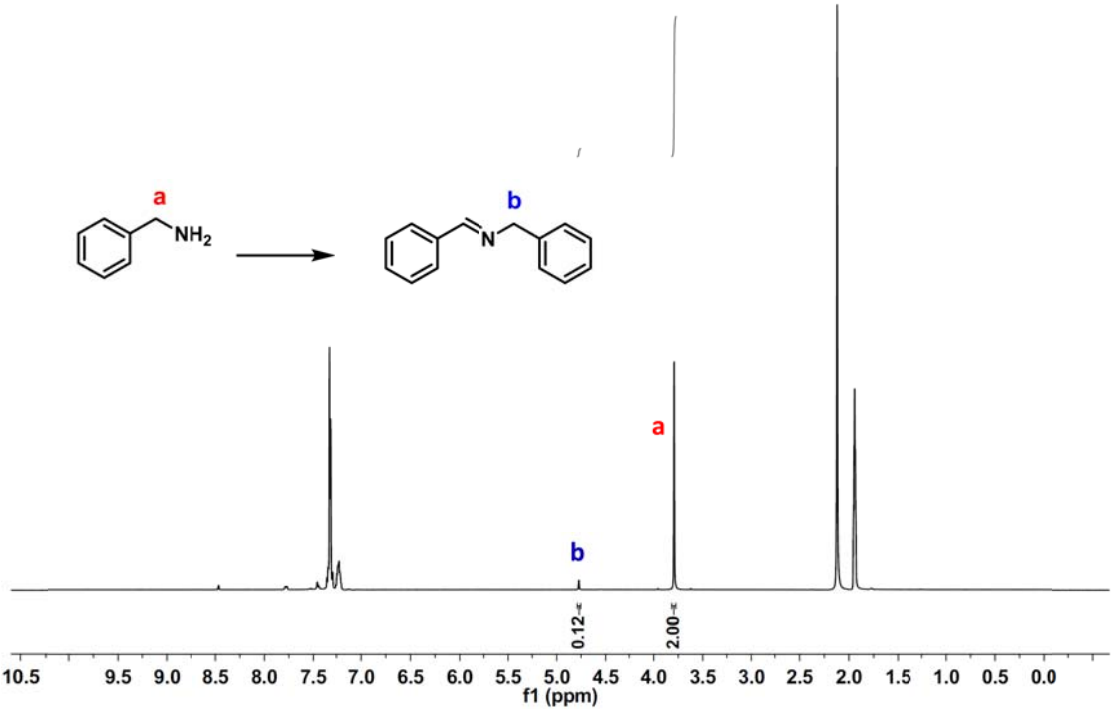

Fig. S19 ^{1}H NMR of the reaction mixture (Entry 5, Table 1).

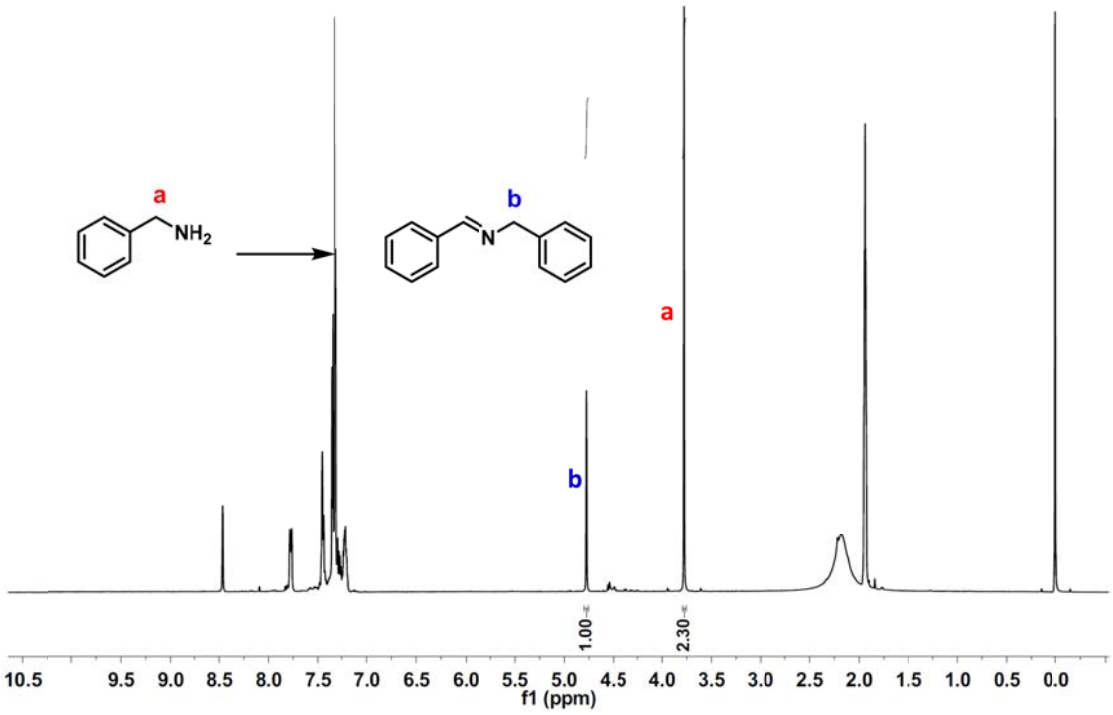

Fig. S20 ^{1}H NMR of the reaction mixture (Entry 6, Table 1).

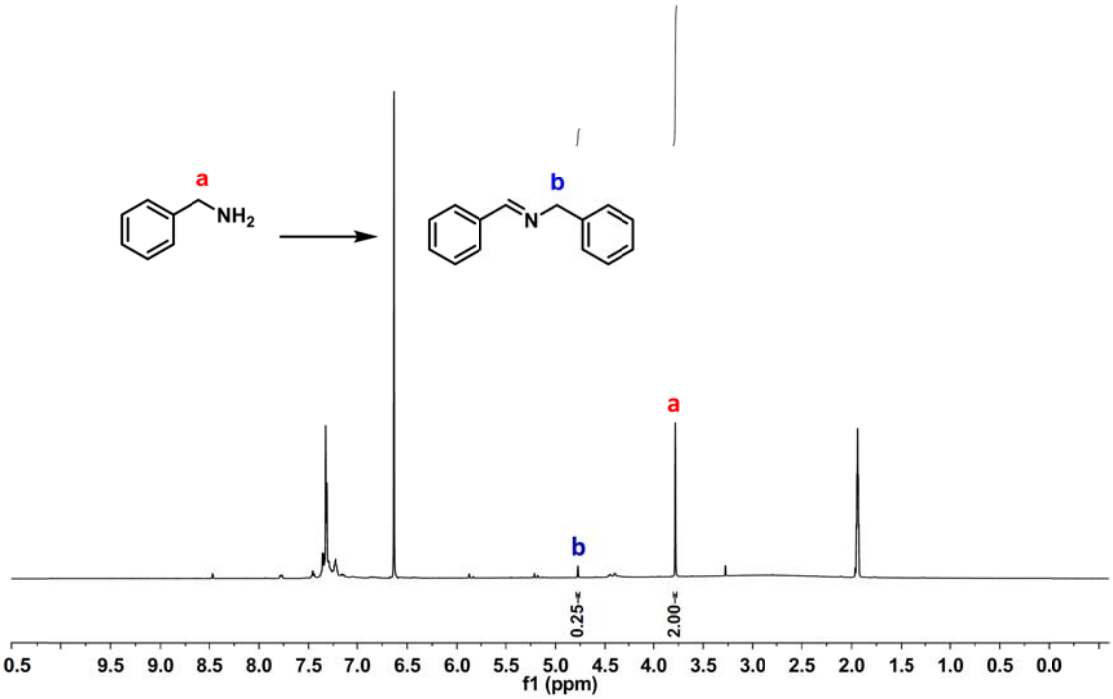

Fig. S21 ^{1}H NMR of the reaction mixture (Entry 7, Table 1).

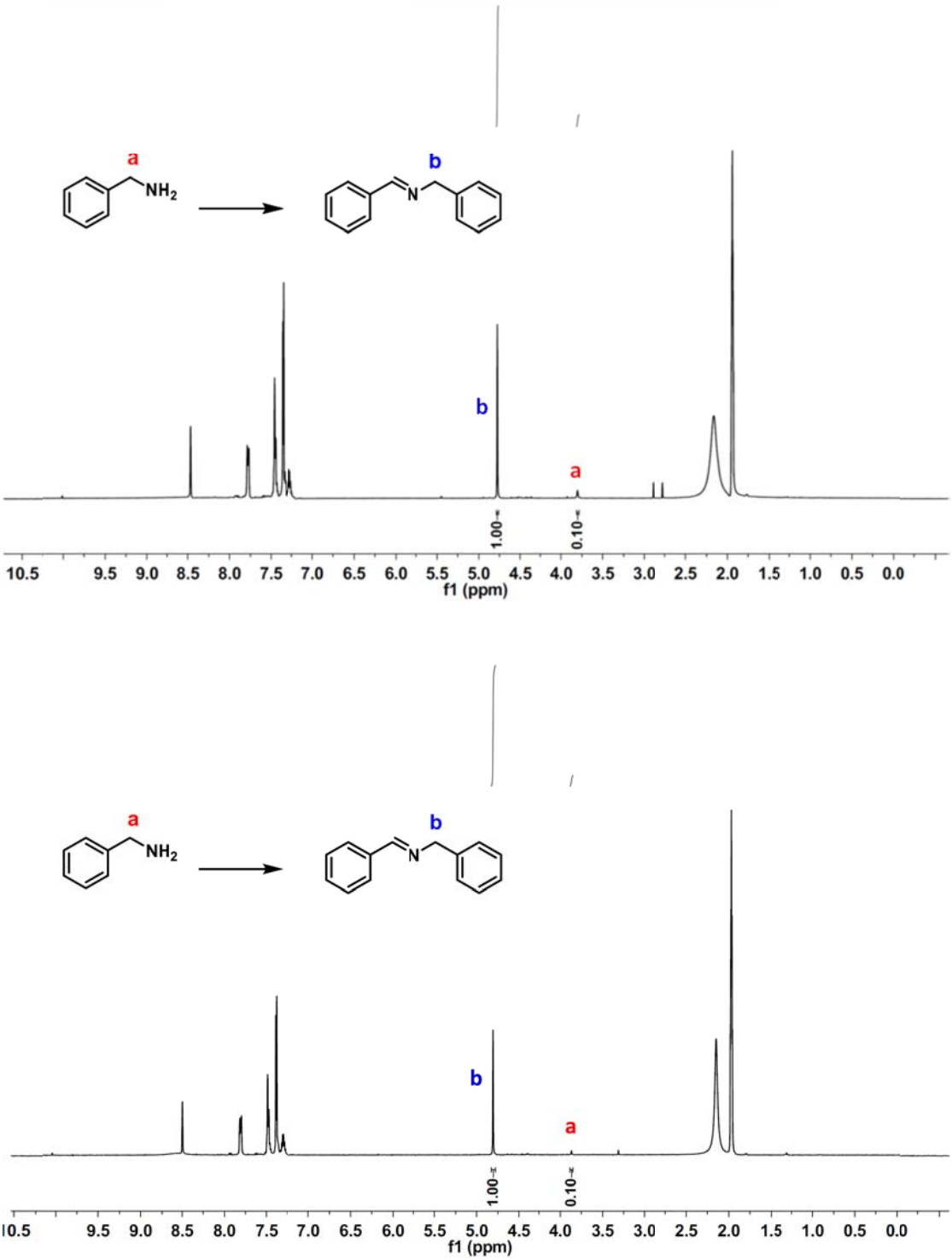

Fig. S22 ^{1}H NMR of the reaction mixture after photocatalysis by TpTc-POP (upper, Entry 1, Table 2) and TbTc-POP (bottom, Entry 1, Table S1).

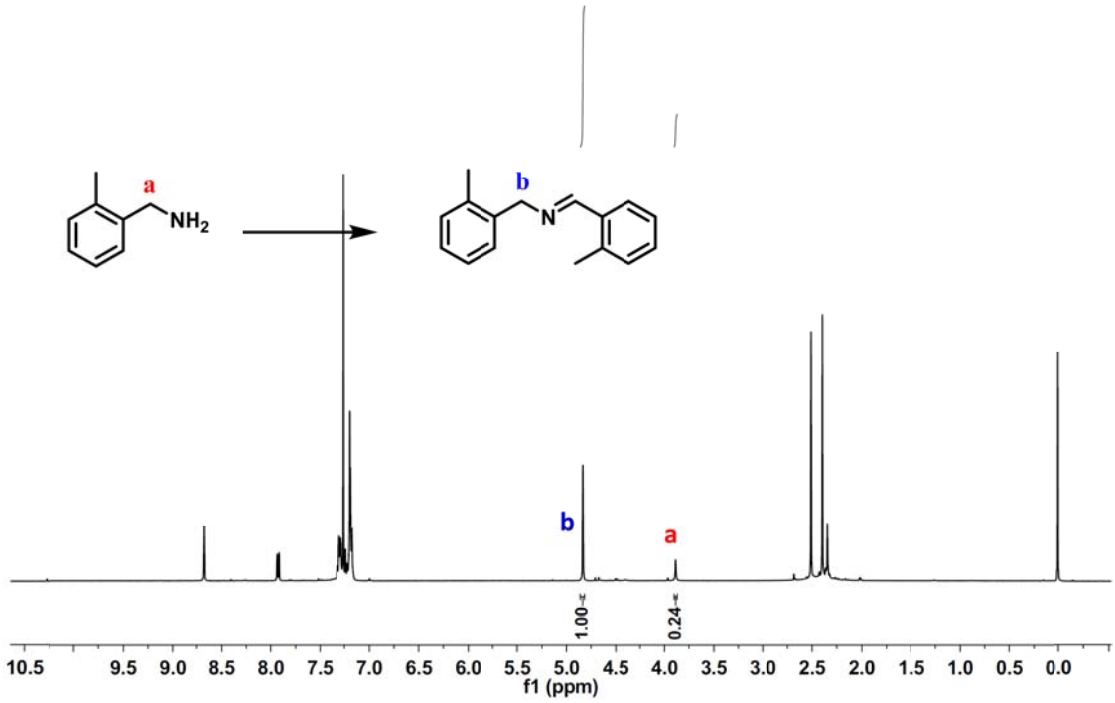

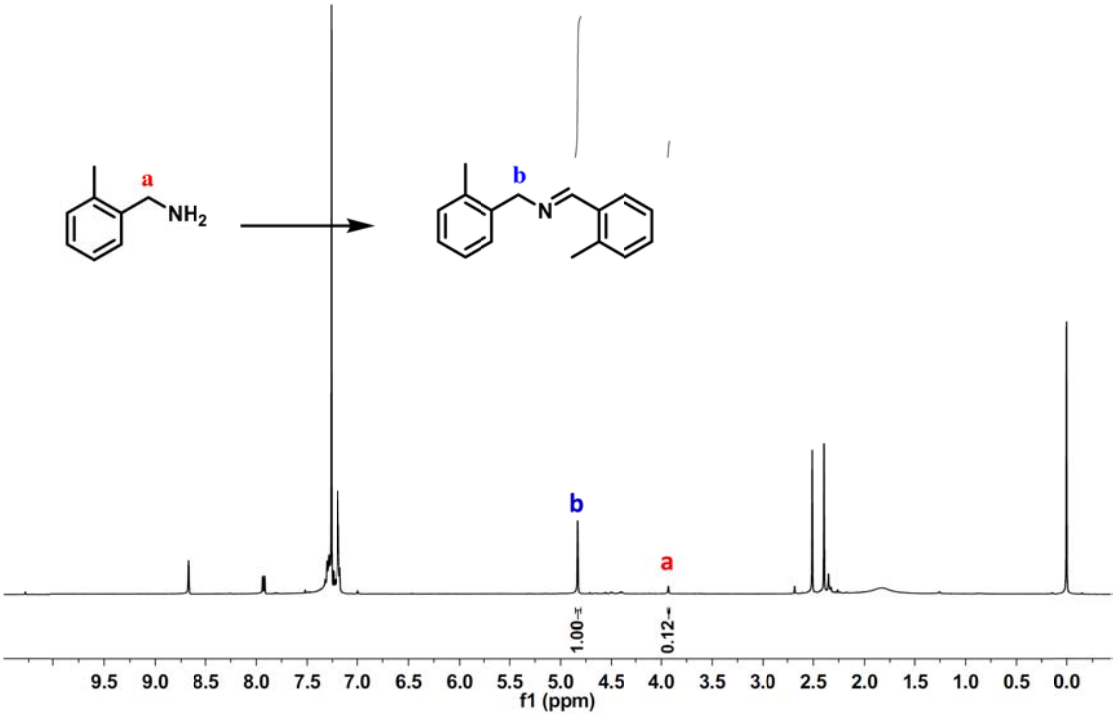

Fig. S23 ^{1}H NMR of the reaction mixture after photocatalysis by TpTc-POP (upper, Entry 2, Table 2) and TbTc-POP (bottom, Entry 2, Table S1).

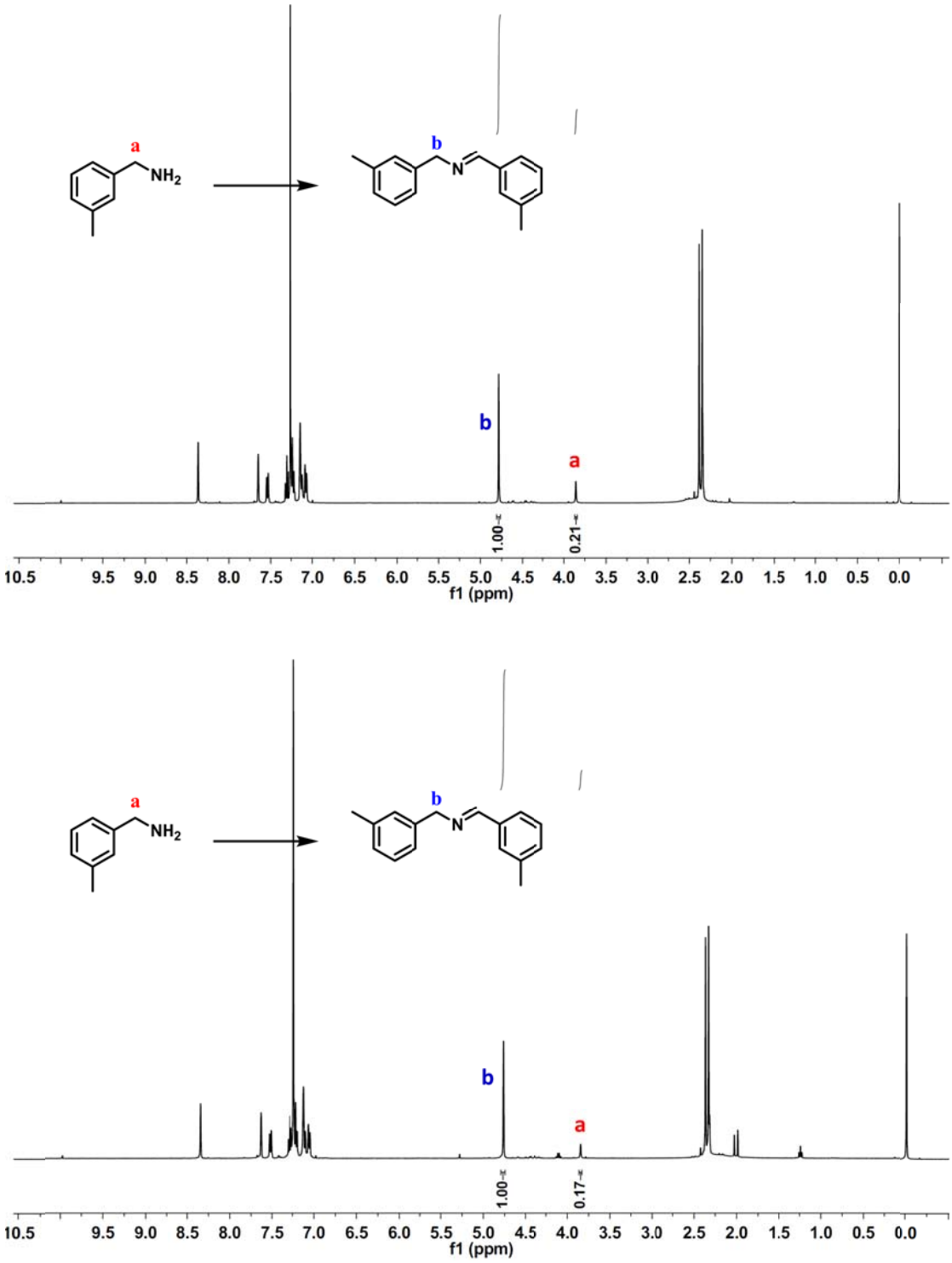

Fig. S24 ^{1}H NMR of the reaction mixture after photocatalysis by TpTc-POP (upper, Entry 3, Table 2) and TbTc-POP (bottom, Entry 3, Table S1).

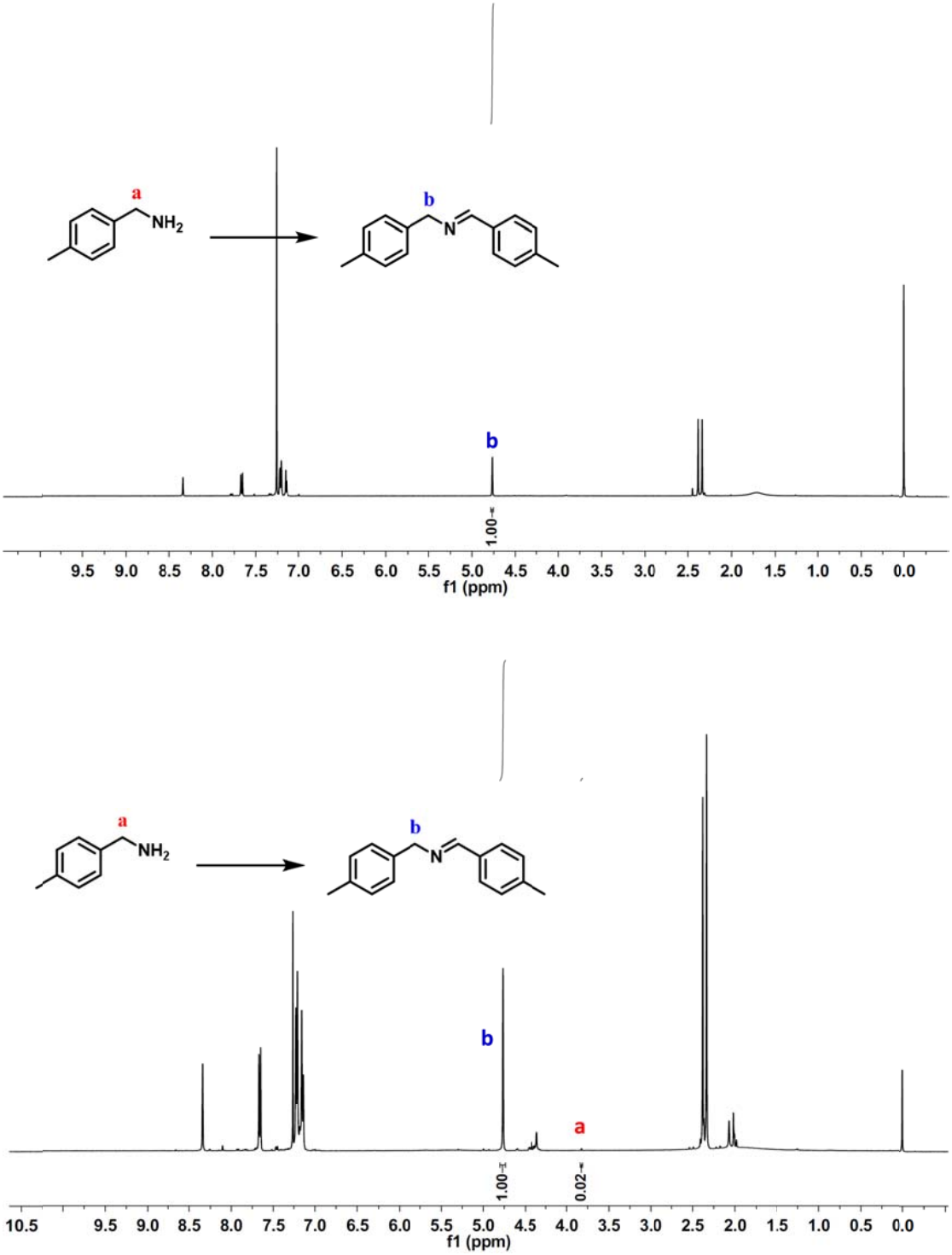

Fig. S25 ^{1}H NMR of the reaction mixture after photocatalysis by TpTc-POP (upper, Entry 4, Table 2) and TbTc-POP (bottom, Entry 4, Table S1).

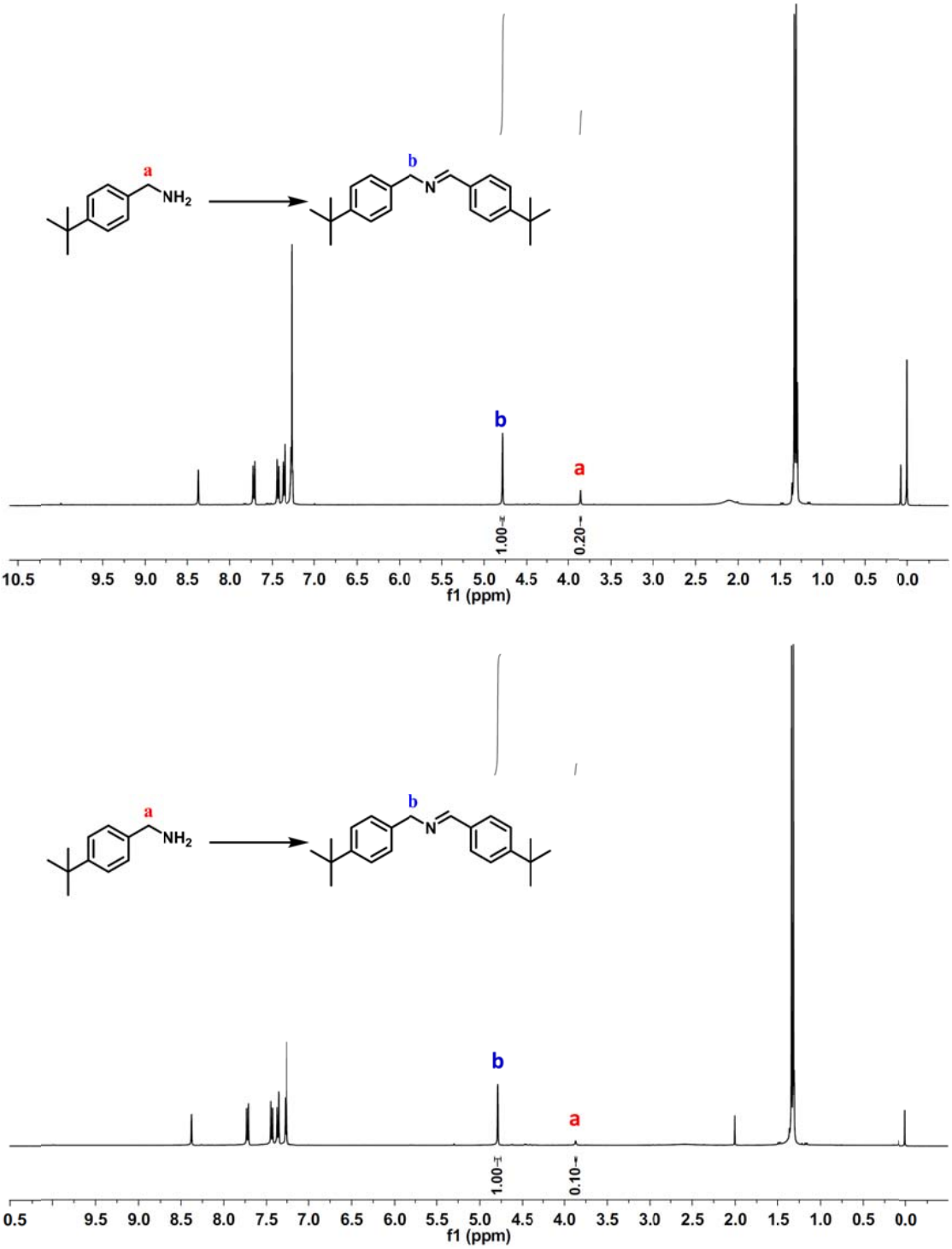

Fig. S26 ^{1}H NMR of the reaction mixture after photocatalysis by TpTc-POP (upper, Entry 5, Table 2) and TbTc-POP (bottom, Entry 5, Table S1).

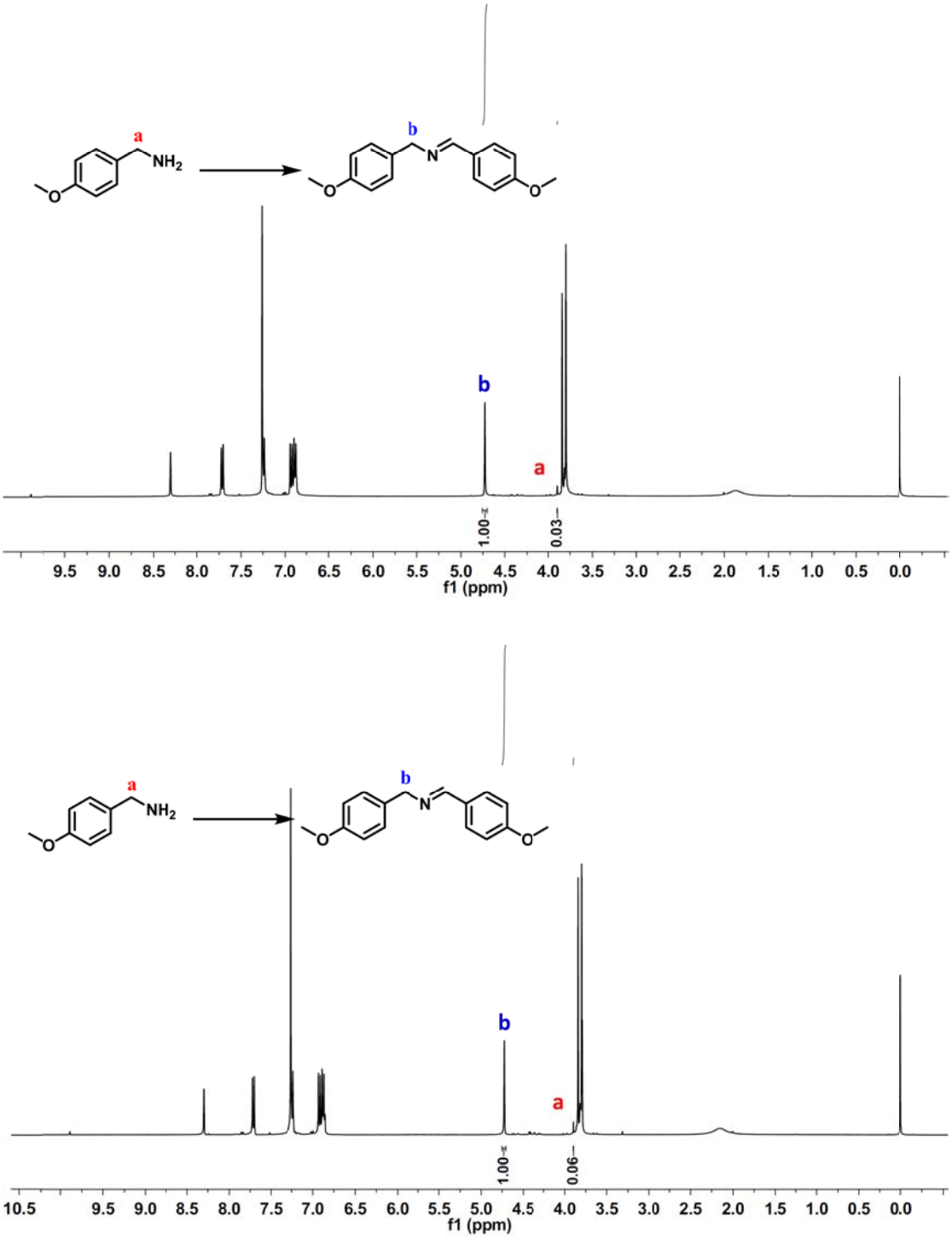

Fig. S27 ^{1}H NMR of the reaction mixture after photocatalysis by TpTc-POP (upper, Entry 6, Table 2) and TbTc-POP (bottom, Entry 6, Table S1).

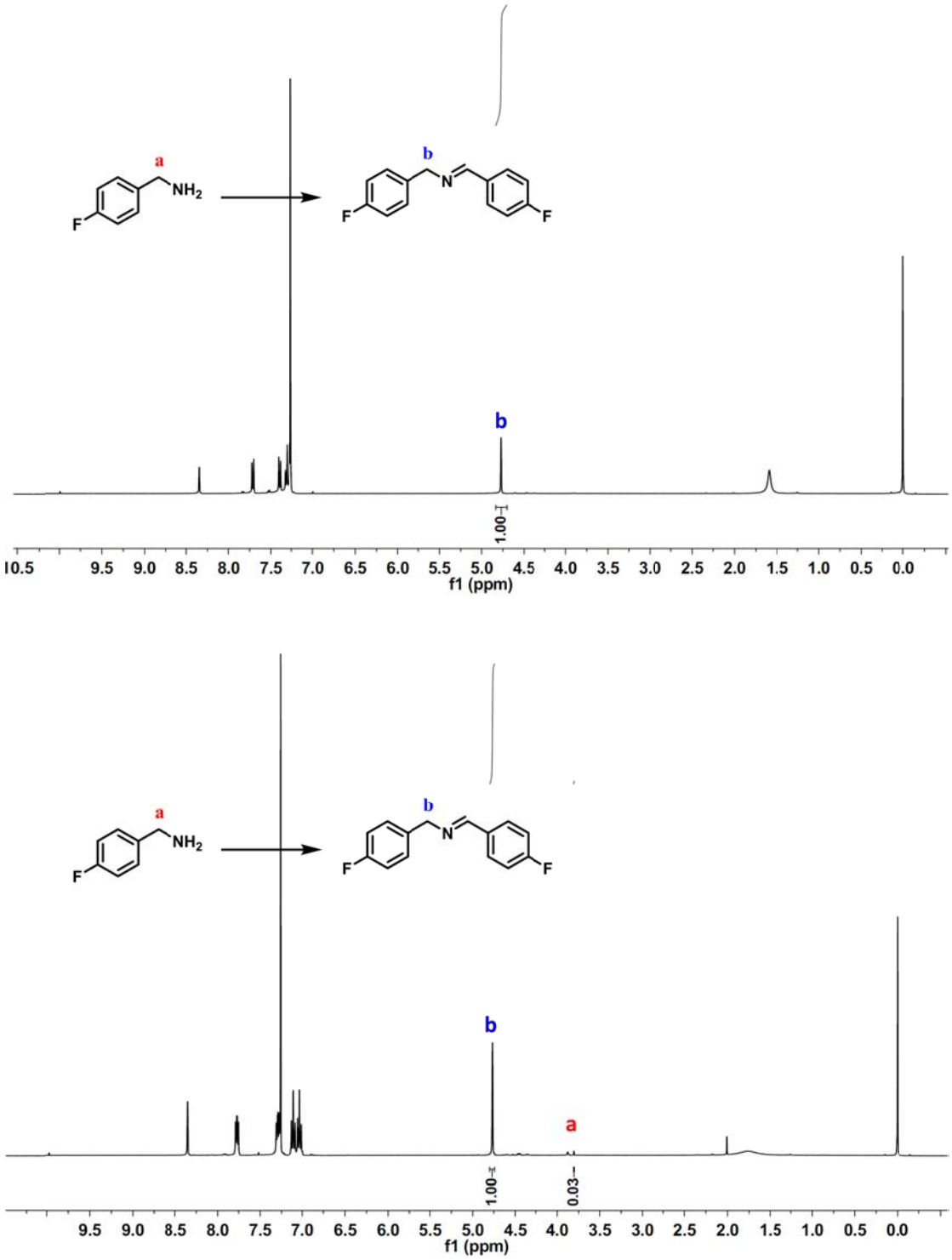

Fig. S28 ^{1}H NMR of the reaction mixture after photocatalysis by TpTc-POP (upper, Entry 7, Table 2) and TbTc-POP (bottom, Entry 7, Table S1).

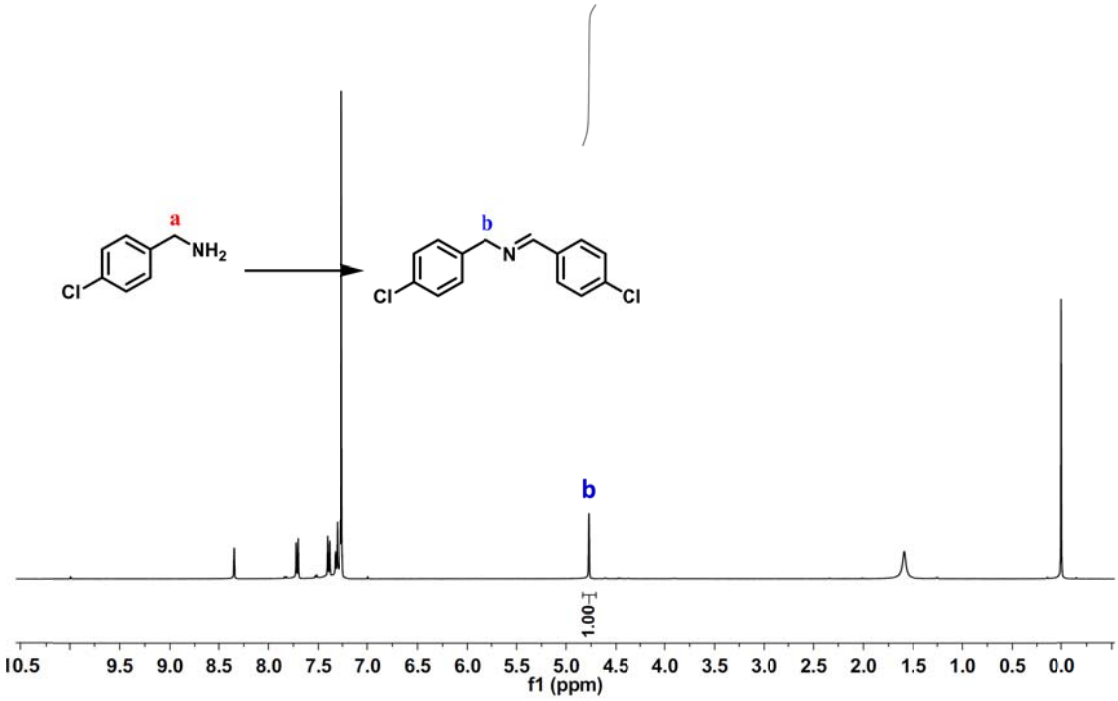

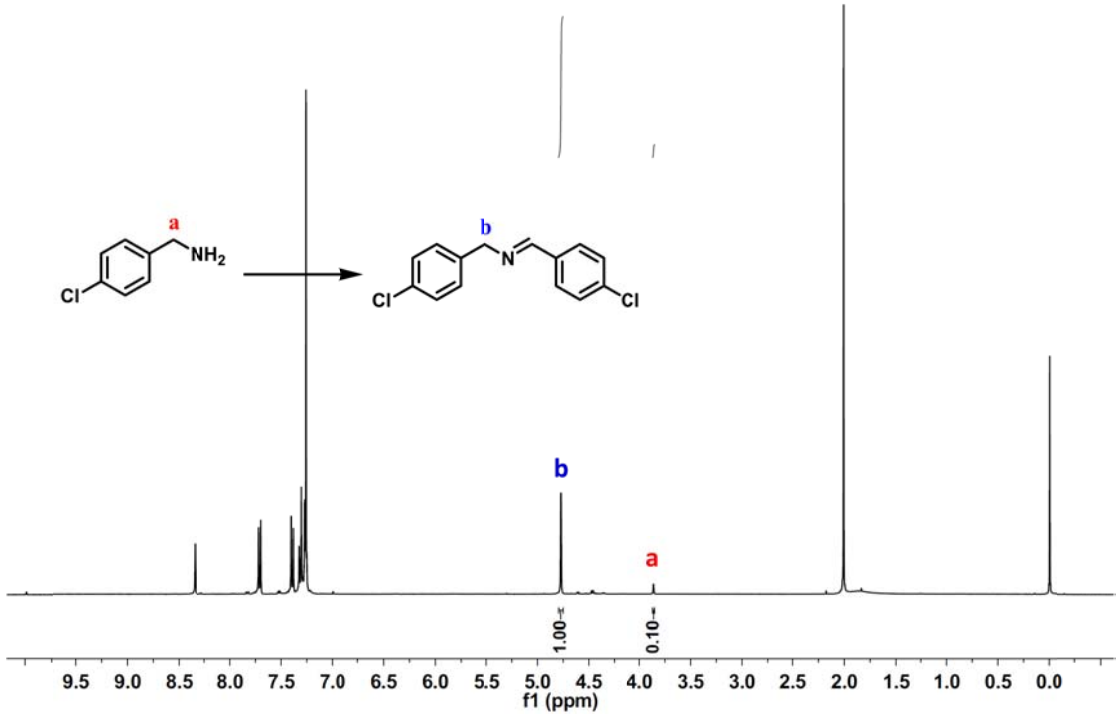

Fig. S29 ^{1}H NMR of the reaction mixture after photocatalysis by TpTc-POP (upper, Entry 8, Table 2) and TbTc-POP (bottom, Entry 8, Table S1).

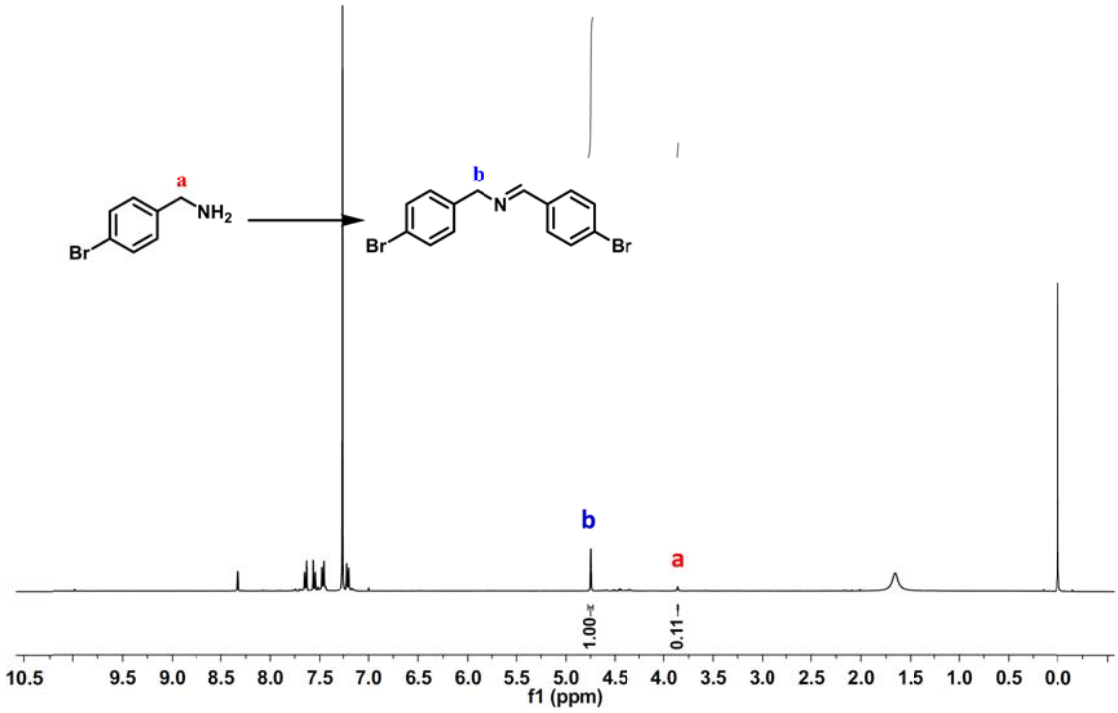

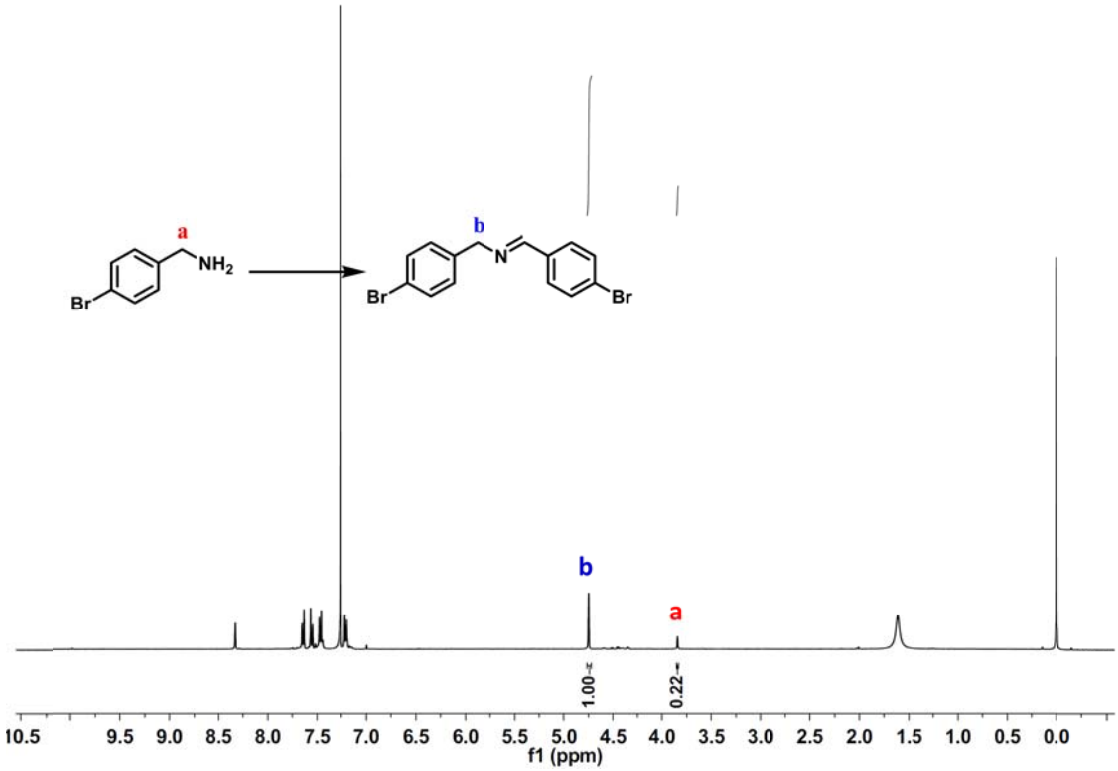

Fig. S30 ^{1}H NMR of the reaction mixture after photocatalysis by TpTc-POP (upper, Entry 9, Table 2) and TbTc-POP (bottom, Entry 9, Table S1).

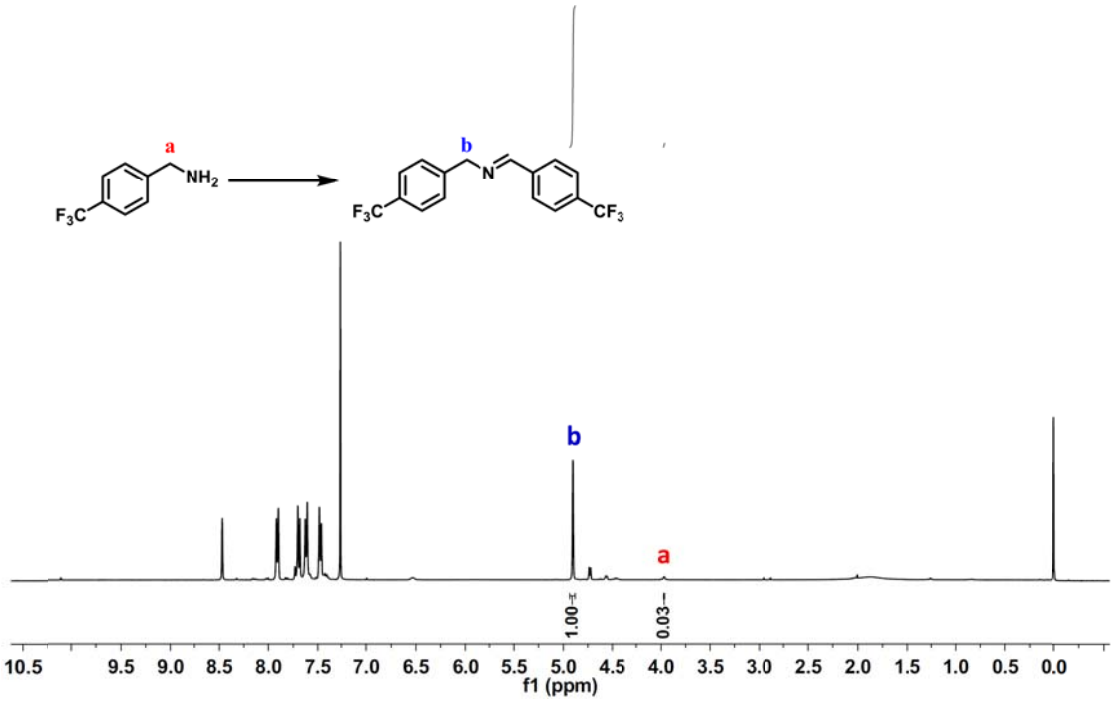

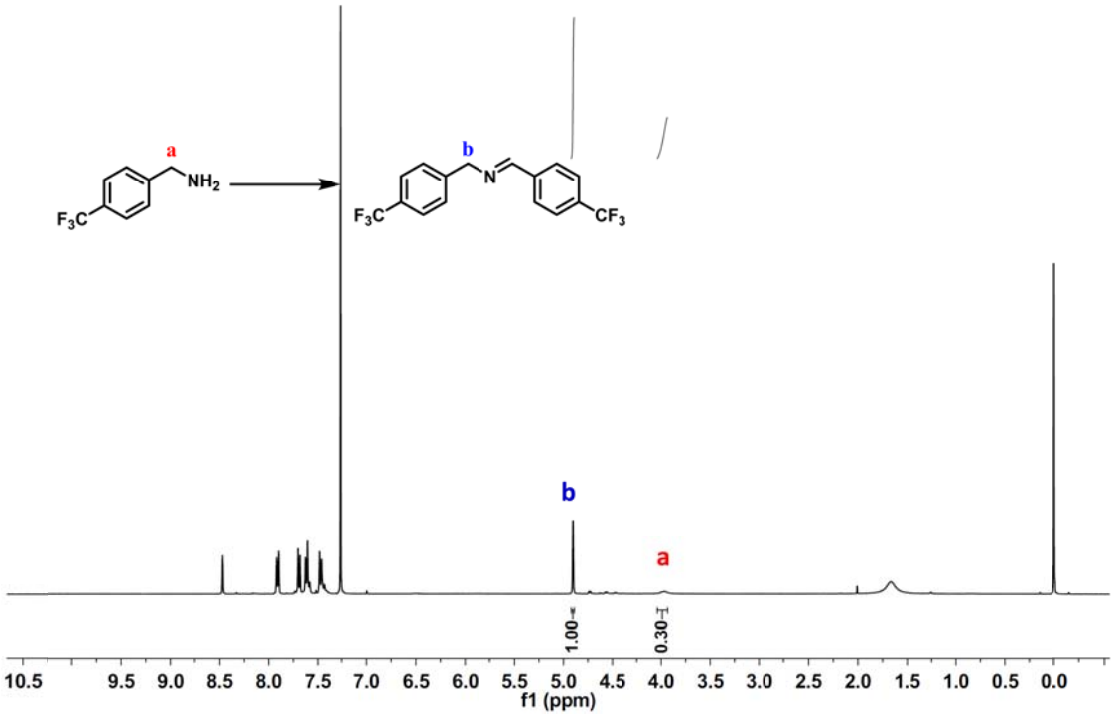

Fig. S31 ^{1}H NMR of the reaction mixture after photocatalysis by TpTc-POP (upper, Entry 10, Table 2) and TbTc-POP (bottom, Entry 10, Table S1).

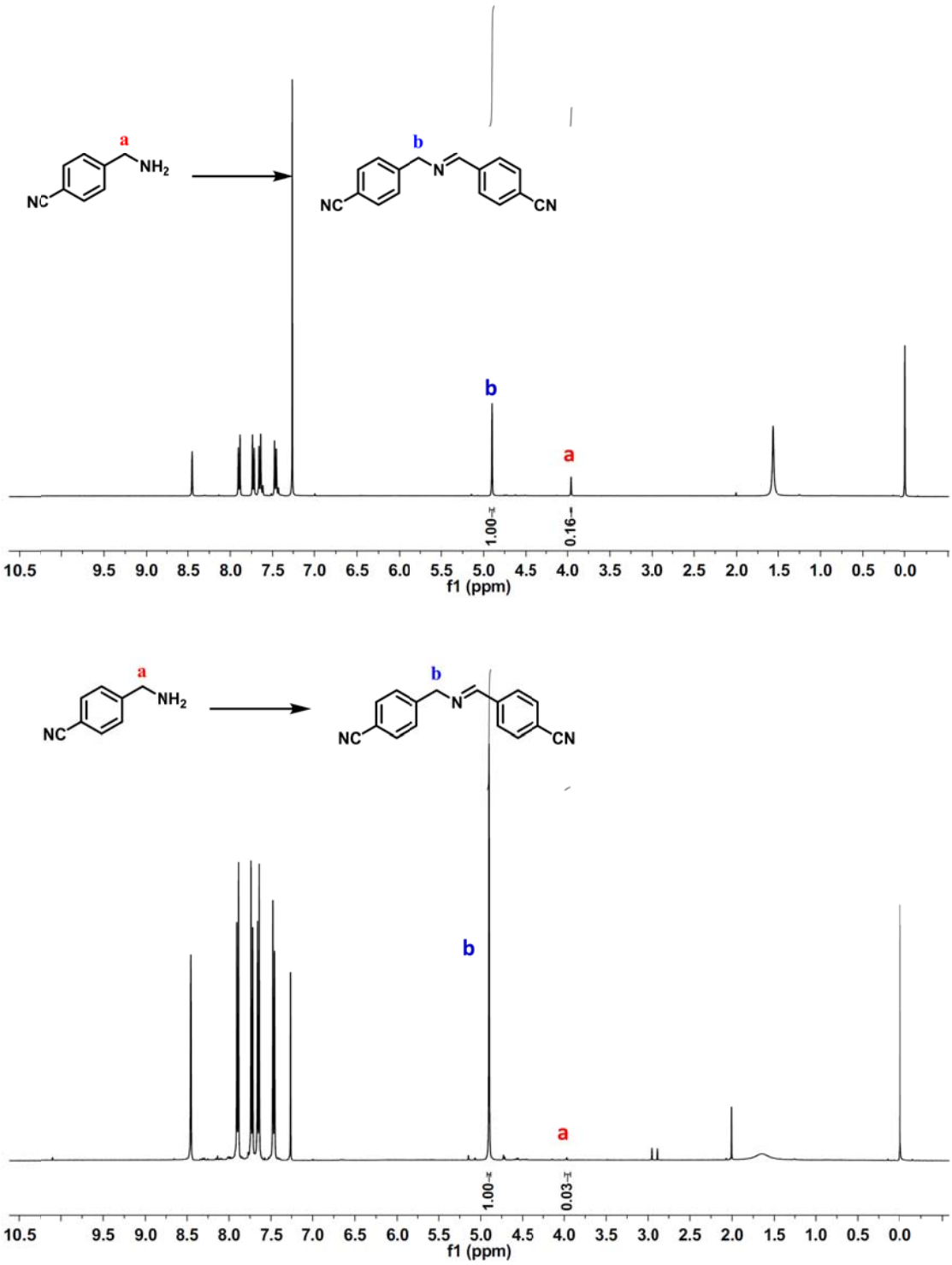

Fig. S32 ^{1}H NMR of the reaction mixture after photocatalysis by TpTc-POP (upper, Entry 11, Table 2) and TbTc-POP (bottom, Entry 11, Table S1).

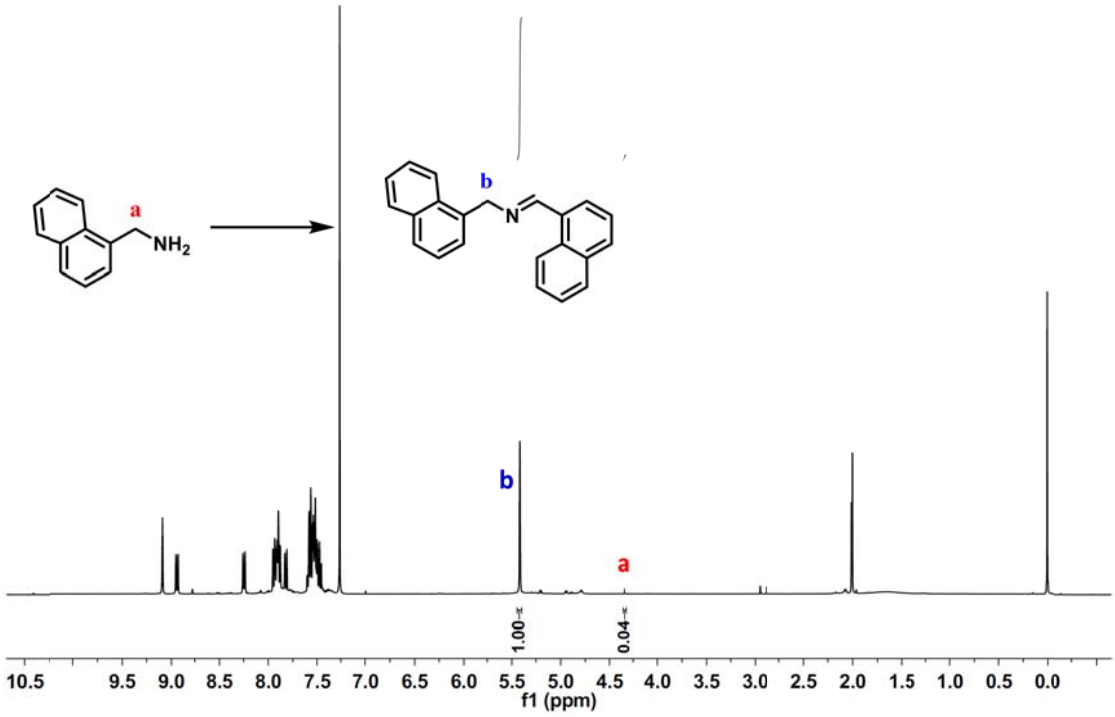

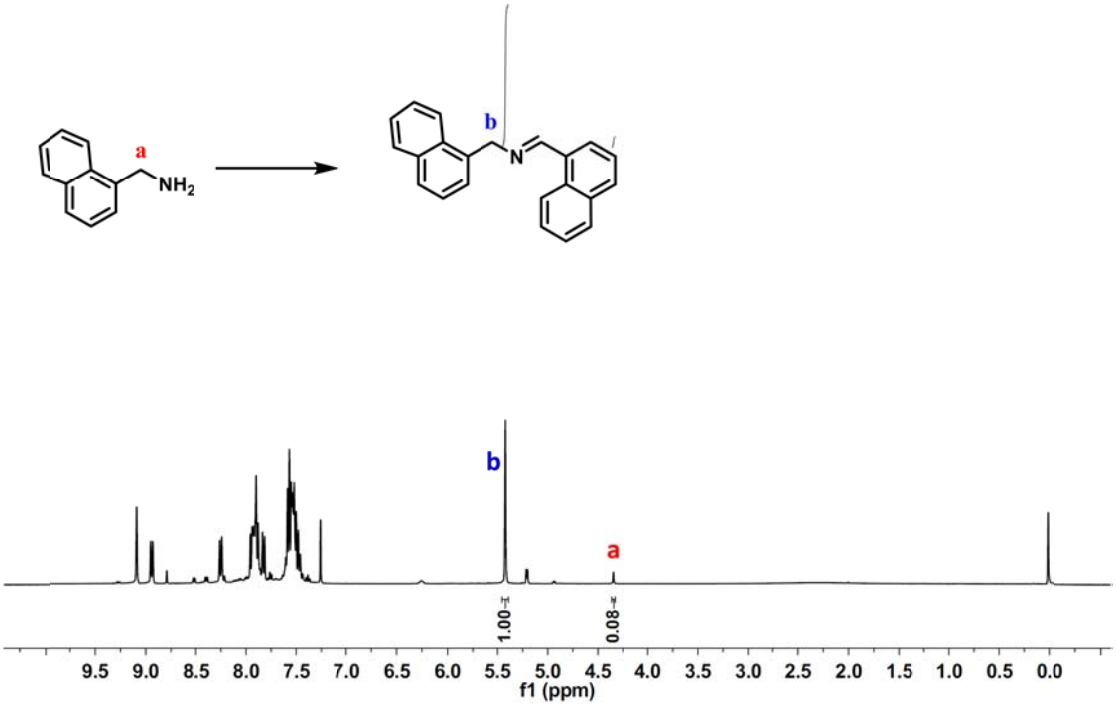

Fig. S33 ^{1}H NMR of the reaction mixture after photocatalysis by TpTc-POP (upper, Entry 12, Table 2) and TbTc-POP (bottom, Entry 12, Table S1).

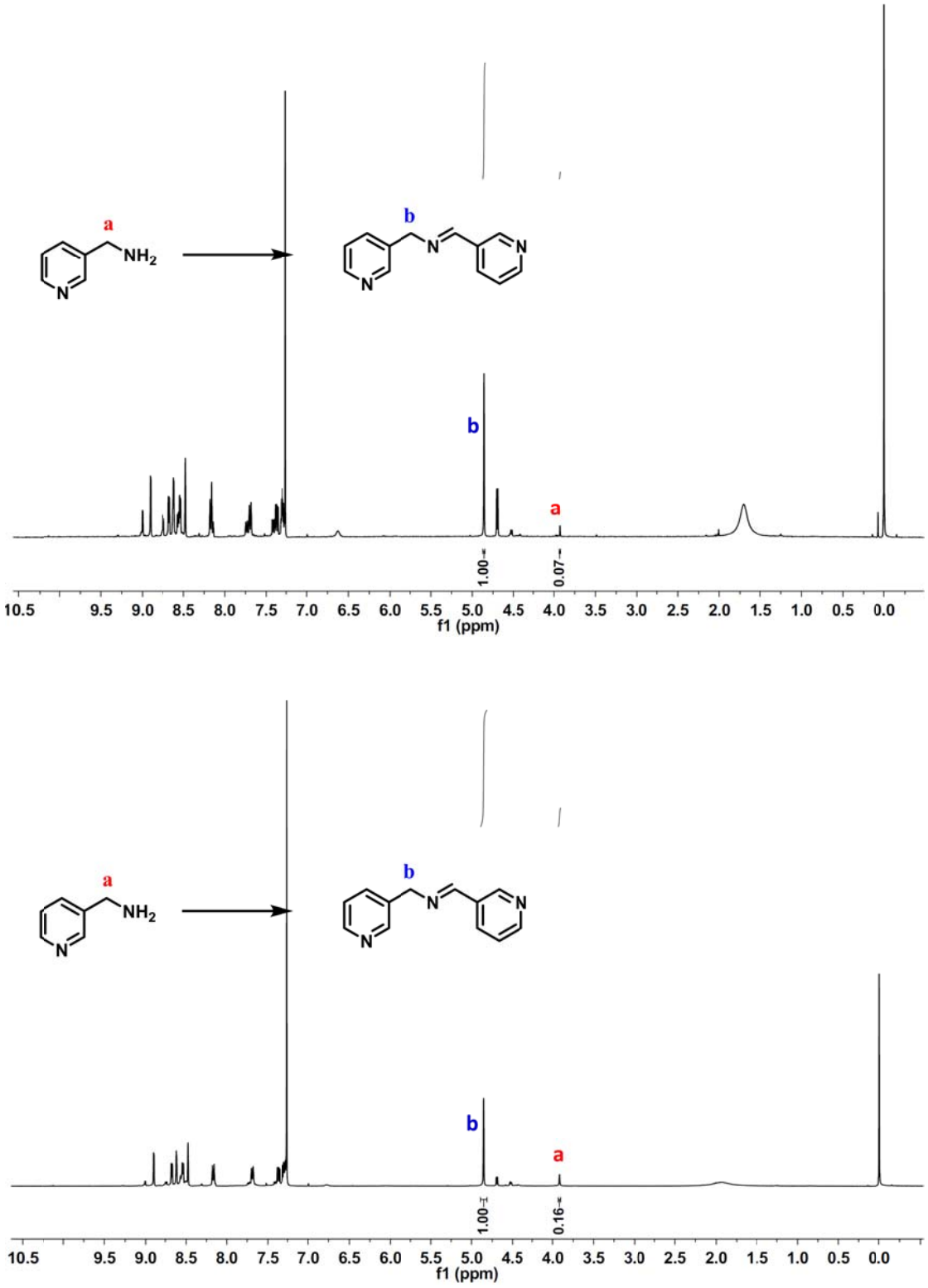

Fig. S34 ^{1}H NMR of the reaction mixture after photocatalysis by TpTc-POP (upper, Entry 13, Table 2) and TbTc-POP (bottom, Entry 13, Table S1).

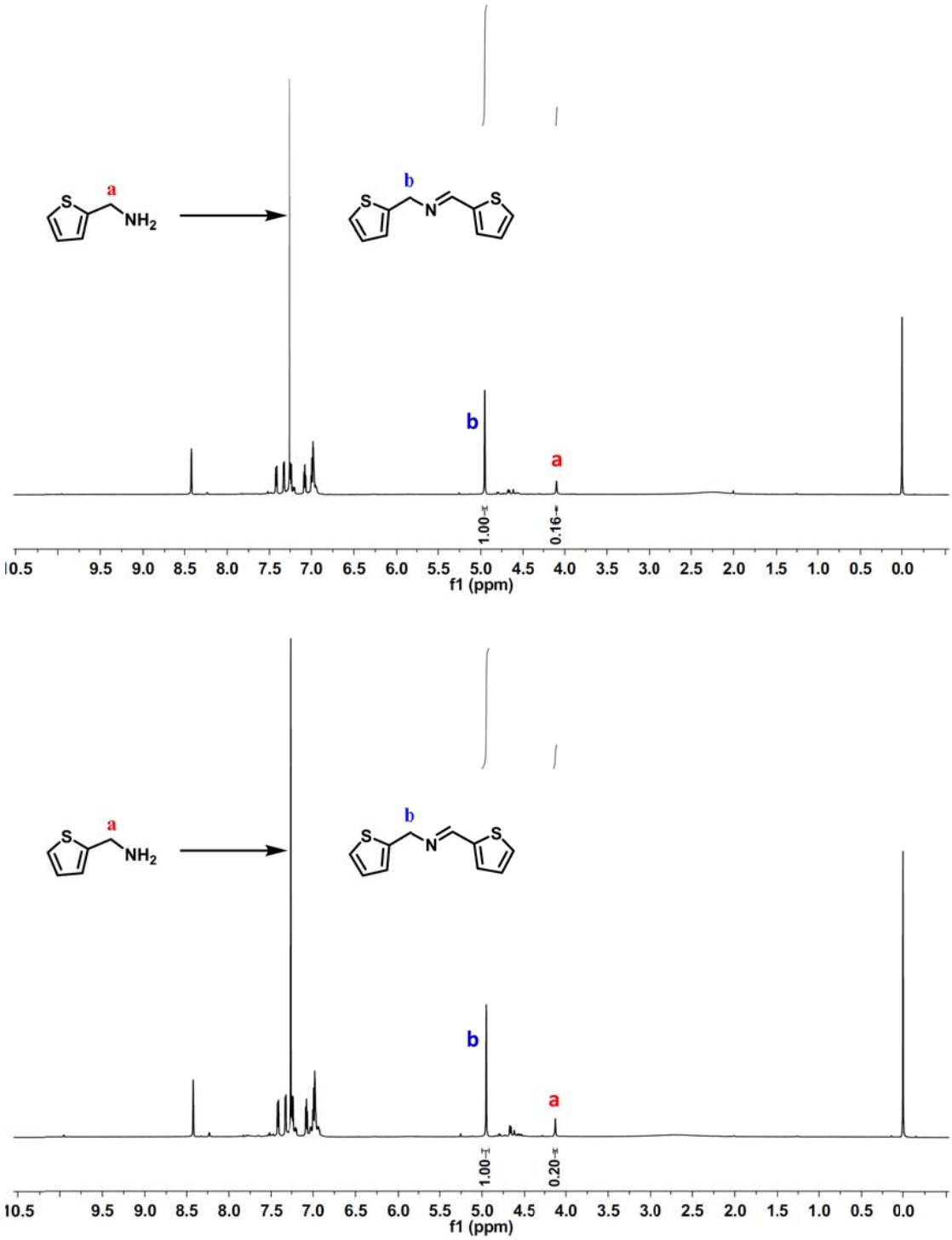

Fig. S35 ^{1}H NMR of the reaction mixture after photocatalysis by TpTc-POP (upper, Entry 14, Table 2) and TbTc-POP (bottom, Entry 14, Table S1).

References

S1 (a) S. Bi, Z.-A. Lan, S. Paasch, W. Zhang, Y. He, C. Zhang, F. Liu, D. Wu, X. Zhuang, E. Brunner, X. Wang and F. Zhang, *Adv. Funct. Mater.*, 2017, **27**, 1703146; (b) B. Jędrzejewska, M. Gordel, J. Szeremeta, P. Krawczyk and M. Samoć, *J. Org. Chem.*, 2015, **80**, 9641-9651.

S2 Y. Zhi, K. Li, H. Xia, M. Xue, Y. Mu and X. Liu, *J. Mater. Chem. A*, 2017, **5**, 8697-8704.

S3 S. Li, L. Li, Y. Li, L. Dai, C. Liu, Y. Liu, J. Li, J. Lv, P. Li and B. Wang, *ACS Catal.*, 2020, **10**, 8717-8726.

S4 X. Lan, X. Liu, Y. Zhang, Q. Li, J. Wang, Q. Zhang and G. Bai, *ACS Catal.*, 2021, **11**, 7429-7441.

S5 W. Li, X. Huang, T. Zeng, Y. A. Liu, W. Hu, H. Yang, Y.-B. Zhang and K. Wen, *Angew. Chem. Int. Ed.*, 2021, **60**, 1869-1874.

S6 J.-L. Shi, R. Chen, H. Hao, C. Wang and X. Lang, *Angew. Chem. Int. Ed.*, 2020, **59**, 9088-9093.

S7 J. Luo, J. Lu and J. Zhang, *J. Mater. Chem. A*, 2018, **6**, 15154-15161.

S8 Z. J. Wang, K. Garth, S. Ghasimi, K. Landfester and K. A. I. Zhang, *ChemSusChem*, 2015, **8**, 3459-3464.

S9 Z. J. Wang, S. Ghasimi, K. Landfester and K. A. I. Zhang, *Adv. Mater.*, 2015, **27**, 6265-6270.

S10 S. Bandyopadhyay, S. Kundu, A. Giri and A. Patra, *Chem. Commun.*, 2018, **54**, 9123-9126.